THESIS FOR THE DEGREE OF DOCTOR OF PHILOSOPHY

Mass Transport in Wood Disintegration:

Implications for the Pulp and Paper Industry

ROUJIN GHAFFARI

Department of Chemistry and Chemical Engineering

CHALMERS UNIVERSITY OF TECHNOLOGY

Gothenburg, Sweden 2023

Mass Transport in Wood Disintegration:
Implications for the Pulp and Paper Industry

ROUJIN GHAFFARI
ISBN: **978-91-7905-929-3**
Series number: **5395**

Doktorsavhandlingar vid Chalmers tekniska högskola
Ny serie nr (ISSN0346-718X)

Department of Chemistry and Chemical Engineering
Chalmers University of Technology
SE-412 96 Gothenburg
Sweden
Telephone + 46 (0)31-772 1000

I, Roujin Ghaffari, hereby certify that this thesis is my original work and, to the best of my knowledge, does not contain any material previously published or written by another person, except where due reference or acknowledgement is made.

Cover: The image depicts important mass transport steps in the separation of wood building blocks, designed and generated using Blender software.

Printed by:

Chalmers Digitaltryck

Gothenburg, Sweden 2023

Mass Transport in Wood Disintegration:

Implications for the Pulp and Paper Industry

Roujin Ghaffari

Department of Chemistry and Chemical Engineering

Chalmers University of Technology

Abstract

Efficient delignification and fractionation processes are essential in the pulp and paper industry. Mass transport events in wood fractionation are of great importance, specifically in two main stages, namely, the mass transport of chemicals into wood and the mass transport of degraded lignin molecules out of cellulose confinements. It has been previously suggested that the mass transport of lignin molecules through fibers is the rate-determining step in kraft pulping. This thesis first investigates the effects of pore sizes, the alkalinity of the solution, the molecular weight of lignin, and specific ion effects on the mass transport of lignin through model cellulose membranes using diffusion cells. Furthermore, the adsorption of lignin on cellulose substrates in the presence of salts chosen from the Hofmeister series was studied using a quartz crystal microbalance with dissipation monitoring (QCM-D). It was observed that mass transport rates through the cellulose membrane were enhanced by an increase in pore size, alkalinity of the solution, and a decrease in lignin molecular weight. Higher alkalinity of the solution decreases the association between the lignin molecules, which increases the mass transport. QCM-D measurements showed that the adsorption of lignin on cellulose was increased in the presence of chaotropic anions. This behavior can be rationalized by the system's entropy gain, facilitated by the release of adsorbed ions and water molecules from the cellulose surface upon lignin adsorption. The thesis also explores the rate-determining step in the ionoSolv fractionation process. To achieve a more homogeneous fractionation, the effects of temperature, water content, and vacuum on the impregnation of wood by ionic liquids (ILs) were further studied. This thesis not only highlights the complexity of mass transport events in wood fractionation but, by comparing the concentration of lignin released from dry wood, IL-impregnated wood, and previously reacted wood samples over time, has also revealed that the mass transport of the IL into wood is the rate-determining step.

Keywords: Kraft pulping, delignification, mass transport, specific ion effects, ionic liquids, ionoSolv, impregnation

"What I love about science is that as you learn, you don't really get answers. You just get better questions."

John Green

To my loving family

List of Articles

This thesis is based on the work contained in the following articles:

1. **Mass transport of lignin in confined pores**
   Roujin Ghaffari, Henrik Almqvist, Robin Nilsson, Gunnar Lidén, Anette Larsson
   Polymers **2022**, *14*(10), 1993; https://doi.org/10.3390/polym14101993

2. **Effect of alkalinity on the diffusion of solvent-fractionated lignin through cellulose membranes**
   Roujin Ghaffari, Henrik Almqvist, Alexander Idström, Ioanna Sapouna, Lars Evenäs, Gunnar Lidén, Martin Lawoko, Anette Larsson
   Cellulose 30, 3685–3698 (2023). https://doi.org/10.1007/s10570-023-05098-8

3. **Specific ion effects on lignin adsorption and transport through cellulose confinements**
   Roujin Ghaffari, Vishnu Arumughan, Anette Larsson
   Accepted for publication in the Journal of Colloids and Interfaces, 2023.
   https://doi.org/10.1016/j.jcis.2023.09.037

4. **Mass transport of ionic liquids into wood**
   Roujin Ghaffari, Agnieszka Brandt-Talbot, Anette Larsson
   Manuscript

Contribution Report

1. Main Author. Designed and performed the majority of the experiments and analyzed the data with input from Anette Larsson. Wrote the original draft of the manuscript and reviewed and edited the article with support from Anette Larsson and the other co-authors.

2. Main Author. Designed and performed the experiments and analyzed the data with input from Anette Larsson. Wrote the original draft of the manuscript and reviewed and edited the article with support from Anette Larsson and the other co-authors.

3. Main Author. Designed and performed the experiments and analyzed the data with input from Anette Larsson and Vishnu Arumughan. Wrote the original draft of the manuscript and reviewed and edited the article with support from the co-authors.

4. Main Author. Designed and performed the experiments and analyzed the results with input from Anette Larsson and Agnieszka Brandt-Talbot. Wrote the original draft of the manuscript and reviewed and edited the article with support from the co-authors.

Publications not included in the thesis

1. **Viscoelastic properties of lignin isolated with high yield from softwood kraft pulp, Norway spruce and wheat straw**

   Åke Henrik-Klemens, Fabio Caputo, Roujin Ghaffari, Gunnar Westman, Ulrica Edlund, Lisbeth Olsson, Anette Larsson

   Submitted to Cellulose

2. **Reducing friction between metal and thermo-mechanical pulp using alkyl ketene dimers and magnesium stearate**

   Seyedehsan Hosseini, Roujin Ghaffari, Anette Larsson, Gunnar Westman, Anna Ström

   Manuscript

Abbreviations

AFM	Atomic Force Microscopy
IL	Ionic Liquids
KL	Kraft Lignin
LMWA	Law Of Matching Water Affinities
ML	Middle Lamella
MW	Average Molecular Weight
MWCO	Molecular Weight Cut-Off
QCM-D	Quartz Crystal Microbalance with Dissipation Monitoring
RC	Regenerated Cellulose
SEC	Size Exclusion Chromatography
SEM-EDX	Scanning Electron Microscopy with Energy-Dispersive X-Ray Spectroscopy
TMSC	Trimethylsilyl Cellulose

Table of contents

Chapter 1: Introduction

In an era characterized by evolving environmental concerns, the search for alternative energy sources and materials to replace fossil-based products and decrease greenhouse gas emissions is of utmost importance. Addressing the demands of modern society for renewable resources while reducing adverse environmental impact has highlighted the significant role of sustainable utilization of biomass. Widely available and renewable lignocellulosic biomass presents a platform for the production of nearly closed carbon cycle fuels, chemicals, and materials[1,2].

Utilization of lignocellulosic biomass involves addressing two key challenges. The first is the design of energy-efficient and economically viable methods for breaking down biomass into its constituent polysaccharides and lignin. The second challenge is to design a separation method that recovers and maximizes the value of all components present in the lignocellulosic biomass.

Throughout the years, various separation techniques and pretreatment processes have been developed, from mechanical pulping[3,4] to various chemical pulping[5–8] processes. Kraft pulping is a widely employed method for the separation of lignocellulose, holding a significant share of around 80% of pulping processes in the chemical pulping industry[9]. This method involves the liberation of fibers via the degradation and dissolution of lignin, achieved through the digestion of wood chips under high temperatures and pressures in an alkaline mixture[7].

It has been more than 100 years since Carl F. Dahl invented the kraft process in Germany[10]. Since then, the kraft process has been continuously studied and improved from various aspects[4,11–13]. It has been shown in the literature that the mass transport events in the delignification process are of great importance. Despite its proven importance, surprisingly few studies have addressed the mass

transport of degraded and dissolved lignin molecules out of the fiber wall, hence, current understanding of these events remains limited.

Furthermore, the quest to find novel biomass pretreatment and separation techniques continues. One recently developed processes is the ionoSolv pretreatment process[14–16]. This process utilizes low-cost ionic liquids (ILs) to separate highly digestible cellulose pulp and lignin for further valorization. While this new process has shown great potential for the pretreatment of various biomass feedstocks, its use for wood chips is still under investigation[17,18]. One of the challenges that the ionoSolv process is faced with is the efficient and homogeneous transport of ILs into the porous wood structure.

1.1. Aim and Objective

The primary aim of this thesis is to improve the understanding of mass transport processes within wood separation technologies. The thesis focuses on mass transport events from two different perspectives, namely, the mass transport of dissolved and degraded lignin molecules through fibers (Papers 1-3) and the penetration of chemicals into the wood structure prior to the reactions (Paper 4). Hence, within this thesis, the objectives are:

1) To create and develop various methodologies for studying mass transport in model systems.
2) To investigate how various factors, such as the physiochemical properties of the environment and the diffusing species, influence mass transport.

The content of this thesis is based on four studies, which are referred to as Paper 1 to Paper 4 throughout the thesis. Paper 1 focuses on developing diffusion cell techniques aimed at studying the diffusion of kraft lignin (KL) within model regenerated cellulose (RC) membranes with various pore sizes. Subsequently, Paper 2 uses the developed methodology to explore the impact of varying sodium hydroxide concentrations on the diffusion of fractionated KL across the membrane. Paper 3 combines the diffusion cell techniques with quartz crystal

microbalance with dissipation monitoring (QCM-D) studies to investigate the mass transport of lignin molecules in the presence of salts in the solution. All studies in Paper 1 to Paper 3 are primarily relevant to the kraft pulping process.

Lastly, mass transport events associated with the penetration and diffusion of ILs into wood pieces were studied in Paper 4 using a newly developed methodology. This study is of great importance for further development of the ionoSolv pretreatment process for wood chips. Figure 1 summarizes the appended papers and their scope.

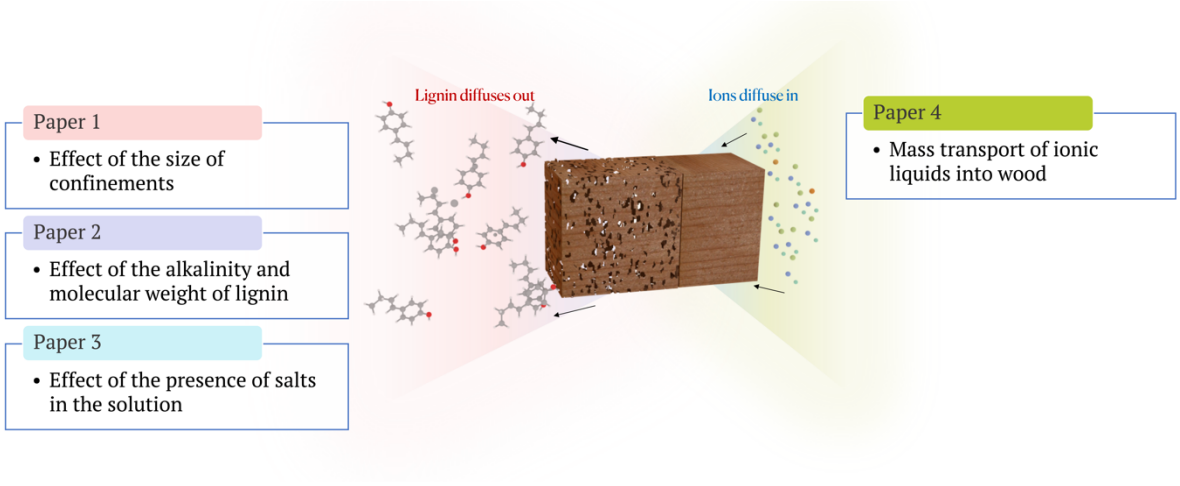

Figure 1 Summary of the appended papers.

The focus of this thesis is mainly within three of the UN sustainable development goals (SDGs):

- Goal number 9 (industry, innovation, and infrastructure): The research aims to advance wood separation technologies by improving the understanding of mass transport processes. This can lead to improvement of the current pulping process and design of more efficient and innovative processes.

- Goal number 12 (responsible consumption and production): This study's focus is on optimizing mass transport processes in wood separation which can promote responsible consumption and production by minimizing waste and use of the resources.

- Goal number 13 (climate action): By developing more efficient wood separation technologies, this research can contribute to reducing the environmental impact of wood processing. Improved processes may lead to reduced energy consumption and lower emissions, thereby supporting climate action.

1.2. Wallenberg Wood Science Center (WWSC)

The thesis is associated with the Wallenberg Wood Science Center (WWSC), an interdisciplinary research hub jointly established by Chalmers University of Technology, The Royal Institute of Technology (KTH), and Linköping University. The WWSC is primarily dedicated to developing novel materials derived from trees and cultivating expertise in the field of sustainable materials for the future. The investigations detailed in this thesis are part of the WWSC's project 1.1.2a, entitled "Mass transport challenges in wood disintegration." This project contributes to enhancing our understanding of the significance and impact of mass transport phenomena within various pulping methodologies.

Chapter 2: Background

Wood has been an important resource for humans from the early ages to modern society[19]. In the early stages of human civilization, wood was mostly used in its natural form with minimum modifications to its chemical structure. For example, wood was used as a source of energy for cooking or heating by burning it as a fuel. Furthermore, early humans used wood to build structures like shelters or cabins and utensils for hunting, like bows or spears[20].

As societies progressed and technological advancements occurred, humans started to modify the chemical structure of wood to utilize it in various applications. This transition marked a significant milestone in the utilization of wood, as it allowed for the production of commodity products with enhanced properties and functionalities. For example, delignified wood pulp was used to produce high-quality paper[21].

In modern society, wood is being used as a feedstock for the production of advanced materials through innovative and sophisticated manufacturing processes. For example, cellulose, one the main components of wood, finds applications in textiles[22,23], as reinforcement material in composites[24,25], or energy storage[26] applications, due to its high strength, good biodegradability, and high aspect ratio when produced as fibers or nanocellulose[27]. Another example is lignin, which was once considered a byproduct of the pulp and paper industry and was mostly burnt to provide energy for the process. Now it can be utilized to produce carbon fibers[28] or bio-based plastics[29].

The growing emphasis on sustainable practices and the replacement of fossil-based resources in recent years has brought even more attention to the utilization of wood and biomass as a renewable feedstock. However, there are several challenges associated with the utilization of wood, including competing with well-

established and cost-effective fossil-based products. Furthermore, the inherently complex structure of wood makes it challenging to separate its building blocks efficiently for their use as a resource for high-value applications.

2.1. Challenges in using biomass

Wood is a highly intricate and heterogeneous material, composed of three main building blocks: cellulose, hemicellulose, and lignin. These building blocks form a highly functionalized matrix. These three main components of wood are interconnected through strong covalent chemical bonds and weaker hydrogen bonds and van der Waals forces. The presence of these bonds forms a recalcitrant structure that is difficult to break down[7].

There has been significant progress in wood separation technologies over the last century. However, achieving efficient separation of these building blocks requires advanced technologies and processes. In this chapter, the complex wood structure and selected separation processes are discussed.

2.2. Wood structure and morphology

Before describing the available pulping processes, it is important to review the morphology and fundamental components of wood. Wood cell walls are composed of the three aforementioned structural components, namely, celluloses, hemicelluloses, and lignin[30].

Among the three cell wall components, cellulose makes the structure framework, comprising about 40% of the wood structure. Cellulose is a linear molecule made up of glucose units. The degree of polymerization in cellulose is approximately 10000 and it can form crystalline and non-crystalline regions along the chains[31]. The chains can be aggregated to form bundles, which have been referred to as microfibrils or elementary fibrils in the literature. Microfibrils can form fibrils, which are the building blocks of large cellulose fibers[7].

Hemicelluloses are branched polysaccharides with a significantly lower degree of polymerization than cellulose (about 50-200)[32]. Contrary to cellulose, hemicelluloses mostly form amorphous structures[7].

Lignin is an aromatic complex molecule of three main interconnected monolignols, namely, coniferyl alcohol, sinapyl alcohol, and P-coumaryl alcohol. The lignin structure comprises various carbon-carbon or ether linkages between the monolignols[33]. In the cell wall, lignin bonds covalently and non-covalently with polysaccharides[34]. This results in the creation of lignin-carbohydrate networks, making the cell wall rigid. This rigidity is essential as it prevents excessive swelling in water, a property crucial for facilitating water transport in wood. In the kraft pulping method, lignin is degraded, solubilized, and removed to obtain high-quality fibers.

The interconnected fibers in wood are held together by the middle lamella (ML), a structural matrix primarily composed of lignin. The concentration of lignin within the ML is notable, however, it only accounts for 20–25% of the total lignin content within the wood, since it is the thinnest layer. The secondary cell wall is the thickest layer, where most of the total lignin can be found. It consists of three layers: inner (S1), middle (S2), and outer (S3). The S2 layer is the thickest of the cell wall layers and it contains well-ordered cellulose fibrils[7]. The secondary cell wall contains pits, which allow for water movement between adjacent tracheids. An illustration of a wood cell wall is presented in Figure 2.

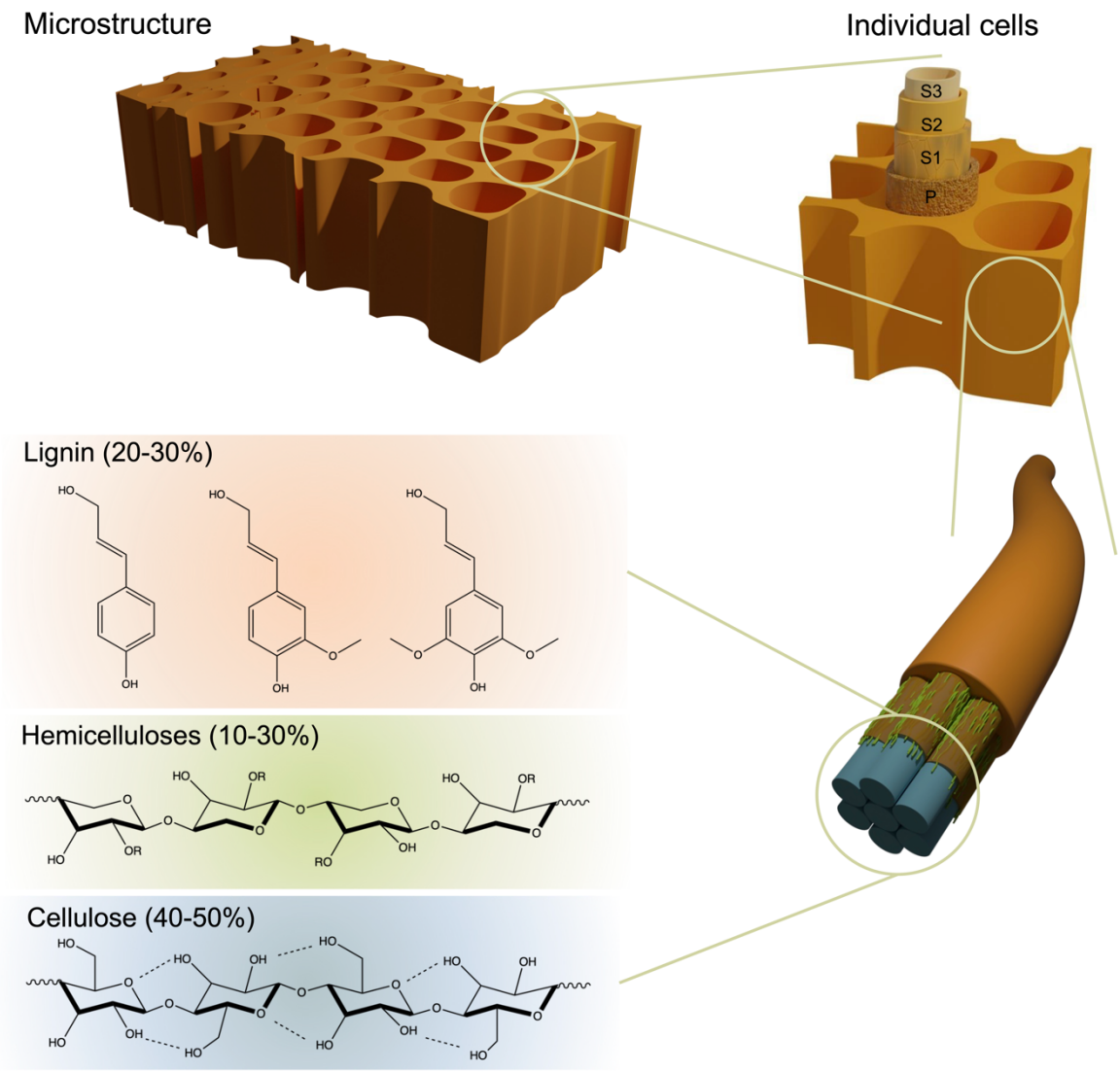

Figure 2 Wood's hierarchical structure and composition. Wood consists of numerous cells primarily oriented longitudinally. Within the lignocellulosic cell wall, there is a primary layer (P) and a secondary layer, the latter of which can be subdivided into S1, S2, and S3 layers. The cell wall is constructed from microfibril bundles. Moreover, wood comprises three key lignocellulosic components: cellulose, hemicellulose, and lignin.

2.3. Overview of the available separation processes

The most established commercial biomass separation processes are kraft and sulfite processes developed for pulp and paper making. These methods were mainly developed to produce high-quality cellulose fibers with high strength. The

lignins produced from these processes are often highly degraded and contain high amounts of sulfur and ash. From the biorefinery perspective, it is desirable to separate all the biomass components for future valorization, which is where other processes have advantages. For example, chemical pretreatment methods based on organic solvents (organosolv method)[6,35], ILs (i.e. ionoSolv)[16,36], and deep eutectic solvents[37] have been widely investigated due to their ability to produce a separate lignin stream for additional applications. This thesis focuses on mass transport events during delignification in the kraft pulping process and the ionoSolv pretreatment method, which is based on the dissolution of lignin by incorporating ILs. In the following sections, these processes are discussed in further detail.

2.3.1. Kraft pulping

Historically, the kraft process is the most common biorefinery process, widely used in the pulp and paper industry. The process involves cooking wood chips at high temperatures and high pressure in a strong alkaline solution, called white liquor. White liquor is a mixture of sodium hydroxide, sodium sulfide, and other ballast chemicals. The liquor penetrates the wood chips, breaks lignin-lignin and lignin-carbohydrate bonds, and dissolves the degraded lignin. The main delignification reaction is the cleavage of ß-aryl bonds in lignin. The dissolved lignin can be removed and recovered from the black liquor (the white liquor that is now enriched with lignin) by filtration or precipitation through various processes such as the LignoBoost process[38]. The resulting pulp from the cook is washed to remove the chemicals and lignin and then further processed to reach the desired brightness. After lignin is removed from the black liquor, white liquor is regenerated from the black liquor through a few recovery steps.

Kraft pulping is performed at temperatures as high as 150-170 °C, and at these temperatures the reactions are completed quickly (within 10-20 minutes)[39], while the cooking is continued for longer times (around 3 hours). At the beginning of the cook, lignin molecules that emerge from the wood structure have lower molecular

weights, while the fractions that are eluted at longer times have higher molecular weights[40]. This is expected as larger lignin molecules have a lower degree of solubility and a lower rate of mass transport out of the cell wall due to their large size. The slow mass transport of lignin out of the porous wood structure is potentially the reason behind the long processing times. The continuous delignification in kraft pulping can ultimately lead to dissolution and loss of carbohydrates, which is not desired. To optimize the yield and quality of pulp high kappa numbers* around 25-30 are considered for softwood[7].

2.3.2. Separation techniques based on ionic liquids

Lignocellulosic biomass pretreatment processes based on ILs are relatively new methods, which initially started with the discovery of cellulose-dissolving ILs. ILs are salts (cations and anions) that are in the form of liquids at or below 100 °C. They have received a significant amount of attention over the past decade, recognized as greener solvents compared to volatile organic solvents[41]. There are two approaches to pretreating biomass with ILs, the first involves dissolution pretreatment, which aims to break down the biomass structure by dissolving cellulose and disrupting its crystalline arrangement[42]. To dissolve cellulose, the presence of robust hydrogen bond accepting anions is essential. The prevalent ILs used for cellulose dissolution typically employ chloride, phosphate, or carboxylate as their anions[43]. Nevertheless, there are drawbacks associated with dissolution pretreatments, including the considerable costs[44] and limited thermal stability of suitable ILs[45], as well as the elevated viscosity of the solution after dissolution of cellulose[36], which adversely affects its processability. Moreover, for effective dissolution pretreatment, the IL's moisture content must be extremely low — a condition that is not practical for biomass separation applications[46,47].

* The kappa number is a measurement used in the pulp and paper industry to quantify the amount of lignin present in wood or pulp.

The other approach involves dissolving and extracting lignin and hemicelluloses, leaving behind a pulp rich in cellulose, such as in the ionoSolv pretreatment. The ionoSolv process is a fractionation process that utilizes low-cost and thermally stable $[HSO_4]^-$-based protic ILs. This process has been successful for a variety of biomass feedstocks such as softwood[48], willow[49], sugarcane[50], coconut husk[51], and Miscanthus[52]. The ionoSolv process, in contrast to dissolution processes, is not sensitive to moisture. In the study conducted by Shi et al.[53], the influence of water in pretreatment using IL-water mixtures was investigated. Water exhibited a dual role as a co-solvent and reduced IL viscosity, aiding in lignin removal. Additionally, water acted as an anti-solvent for cellulose, disrupting the hydrogen-bonding properties of the IL anion and decreasing its attraction to cellulose. When considering ILs that dissolve lignin, the addition of water enhanced lignin solubilization compared to anhydrous conditions[17]. The effectiveness of pretreatment was further enhanced by elevated temperatures for shorter reaction times, optimizing the space-time yield[54]. This process shows great potential for industrialized pulping processes. An initial economic evaluation demonstrated that employing these cost-effective protic ILs for the pretreatment of biomass could result in a financially feasible process[55]. These results suggest that the ionoSolv procedure holds promise for scaling up and eventual commercialization.

2.4. Mass transport in pulping

In the process of removing lignin from the fiber wall, chemical reactions break both internal lignin bonds and bonds between lignin and other components. During cooking, these released lignin molecules are dissolved in the liquor and move out from the fiber wall into the surrounding liquid. To initiate these reactions, reactants like hydroxide and hydrogen sulfide ions (for kraft pulping) or ILs (for ionoSolv) must reach the reaction sites within the wood chips. Initially, the mass transport in the wood is driven by a pressure gradient (advective transport) during the initial impregnation of kraft cooking, but only some of the required chemicals are transported this way. In later stages of impregnation and

cooking, the remaining chemicals diffuse into the wood chips due to the concentration gradient[56]. The sequence of delignification events is as follows[57]:

1. Cooking chemicals move from the bulk liquid to the wood chip's surface.
2. The cooking chemicals are transported to reaction sites within the wood chip through pores, for example, the lumen and pits, as well as cell walls.
3. Delignification reactions occur, leading to the dissolution of lignin and other wood components.
4. Degraded and dissolved reaction products move from the reaction sites to the wood chip's surface through cell walls and pores (the lumen and pits).
5. Degraded products transfer from the wood chip's surface back to the bulk liquid.

The first and second points relate to the mass transport process that occurs before delignification, particularly during the impregnation step. On the other hand, the fourth and fifth points address the mass transport events that follow delignification reactions. Taking these aspects into account, the rate of delignification can be governed by either the mass transport events or the kinetics of chemical reactions[58].

2.4.1. Impregnation

To obtain a homogeneous delignification within a wood chip, a successful impregnation is essential. The primary goal of impregnation is to make sure that the active chemicals fully soak into the chips, obtaining a uniform distribution from the chip's surface to its core. The more uniformly the chemicals are distributed, the more uniform the delignification process becomes during cooking. However, if the movement of chemicals through advection and diffusion is insufficient, the center of the chips might not reach the critical chemical concentration required for delignification. The impregnation step is of great importance in chemical pulping processes where relatively large wood pieces, such as wood chips, are used. The most important parameters influencing impregnation are:

- Chip dimensions: this is the most important factor for the penetration of cooking chemicals, therefore, by using thin wood chips, the diffusion length is decreased, leading to more efficient impregnation[59,60].
- Active chemical concentrations: the driving force for diffusion is the concentration gradient between the middle of the wood chip and the outer liquor, with a higher concentration gradient resulting in more rapid diffusion in capillaries[61,62].
- Temperature: since diffusion or mass transport is the main event in the impregnation process, temperature can affect it to a great extent[63].
- Liquid properties such as viscosity and surface tension: high viscosity of a solution indicates its resistance to flow, which could hinder its penetration into a porous structure[64] and surface tension of a liquid could affect the dissolution or growth of small gas bubbles[65].
- Presence of entrapped air: impregnation can be improved by removing the entrapped air in the porous structure of wood through, for example, pre-steaming the wood chip to replace the air with vapor[66].

In the kraft process, for impregnation, the wood chips are immersed in the cooking liquid containing OH^- and HS^- ions. The impregnation of wood chips with cooking chemicals, for the kraft cooking process, has been extensively studied[64,67–71].

In separation processes based on ILs, the wood pieces should be soaked in viscous IL to be impregnated. The high viscosity of ILs affects the impregnation process significantly. So far, the separation processes based on ILs are limited to the use of saw dust[16], agricultural waste, and perennial plants[51,52], or fine wood particles[72]. On the other hand, size reduction of recalcitrant structures, such as wood, is highly energy intensive[73], therefore, using large particles is more desirable from an economical point of view. In this thesis, the role of mass transport of ILs into wood pieces has been studied, together with how various parameters, such as temperature, water content, or air removal, can affect the impregnation of wood pieces with ILs (Paper 4).

2.4.2. Mass transport of dissolved lignin molecules out of the wood structure

As described earlier, delignification is a complicated process that contains both chemical reactions and physical events such as mass transport. The sequence of mass transport events was provided in section 2.4. In the previous section, the mass transport of chemicals into wood pieces prior to or simultaneous with the reaction was reviewed. In this section, the other mass transport events will be reviewed, namely, the transport of dissolved lignin molecules through the fibers into the lumen and through the lumen to the bulk liquor.

The significance of lignin mass transport in pulping was highlighted in a recent study by Mattsson et al.[39]. Their findings indicated that the majority of delignification reactions conclude within the first 20 minutes of cooking initiation. Nonetheless, the entire cooking process lasts about 3 hours (variable with temperature). This implies that, although reactions reach completion early, the extended cooking duration is necessary to extract the dissolved lignin from fibers into the black liquor. This observation suggests that the mass transport phenomenon outlined in step 4 of section 2.4 could potentially be the rate-limiting step.

In a separate investigation, Brännvall et al.[74] explored the lignin content within both liberated and confined liquor present in the lumen. Comparing these two, the lignin content was found to be lower in the free liquor than in the lumen liquor. Their observations revealed a gradual movement of degraded and dissolved lignin fragments from the lumen liquor to the free liquor. They claimed that the mass transport of lignin from the lumen liquor to the free liquor is possibly hindered by the wood chip's tortuous structure.

These investigations highlight the significance of solubility and mass transport of degraded lignin in the pulping process. Effectively extracting solubilized lignin from the fiber products post-cooking can reduce the need for bleaching[75]. The remaining solubilized lignin within the fiber products can be eliminated (leached

out) during the washing phase. Hence, the mass transport of solubilized lignin from fibers holds importance in this particular step.

In 1981, Favis et al. investigated the leaching of lignin from unbleached kraft fibers suspended in aqueous solutions. Through experimental measurements and theoretical calculations, they determined both the diffusion coefficient of lignin transport through fibers and its theoretical free diffusion coefficient. By comparing these outcomes, they concluded that the rate at which lignin leaches from fibers in aqueous solutions is predominantly regulated by the diffusion of lignin macromolecules[76].

Building on this work, Li et al. conducted a more comprehensive study in 1993, examining the effects of pH, electrolyte concentration, and temperature on the leaching of alkaline lignin from unbleached softwood kraft fibers. Their findings highlighted that higher alkalinity and temperature lead to increased lignin removal. They suggested that the accelerated leaching in alkaline solutions resulted from the dissociation of lignin aggregates into smaller molecules, facilitating easier diffusion through the fibers[77].

Subsequently, Li et al. further explored lignin diffusion from kraft softwood fibers into bulk liquor under alkaline conditions[78]. They extended their investigation to consider the impact of ionic strength and pH. Aligning with their earlier research, they identified a correlation between higher pH and faster diffusion rates. By comparing diffusion rates at pH 12 with ionic strengths of 0.01 M (NaOH) and 0.1 M (0.01 M NaOH and 0.09 M NaCl), they found that larger ionic strengths increased diffusion. This increase in diffusion was attributed to the screening effect on electrostatic interactions between charged lignin and pore walls. As a result, they concluded that factors like pore tortuosity, size, molecular dimensions, and possible electrostatic interactions with pore walls influence the diffusion of lignin.

The significance of mass transport events in delignification processes becomes evident from the aforementioned studies. The diffusion of lignin molecules within cellulose fibers, whether within the lumen or cell walls, can be influenced by various factors such as:

i) Size and molecular weight of the lignin molecules: decreasing the molecular weight of lignin molecules enhances the diffusion coefficient, thereby accelerating the diffusion rate.
ii) Alkalinity of the solution: elevating the pH of the solution reduces the association of lignin molecules, resulting in fewer aggregates in the solution. This leads to an increased diffusion rate.
iii) Ionic strength and the presence of salts in the solution: Diminishing attractive interactions between membrane walls and lignin molecules amplifies their diffusion rate[40,79,80].

In this thesis, the mass transport of lignin molecules in porous confinements of cellulose has been studied with respect to the size of the confinements (Paper 1), the molecular weight of lignin and the alkalinity of the solution (Paper 2), and specific ion effects in the presence of salts (Paper 3).

2.5. Polyelectrolyte adsorption on same charge surfaces

Mass transport of lignin through cellulose fibers is a multifaceted and complicated process. Physicochemical properties of the solution are parameters that can affect lignin's behavior in the solution and its adsorption on the cellulose surfaces. When lignin is adsorbed on the cellulose surface, it creates a layer on the surface of the available spaces in the wood structure, reducing the available space for other molecules to pass through. The surface of cellulose is negatively charged at high pH levels due to the presence of residual wood components such as hemicelluloses or other oxidized groups. Similarly, lignin molecules are negatively charged at high pH levels, which is due to deprotonation of the phenolic and carboxylic groups. Primarily, the interactions between lignin molecules and cellulose surfaces at high pH levels should be governed by electrostatic repulsion. However,

this electrostatic repulsion can be screened by the addition of salts into the solution, thereby promoting adsorption. Scheutjens-Fleer theory about the adsorption of polyelectrolytes on same charged surfaces predicts that, at low salt concentrations, electrostatic repulsion dominates, therefore, no adsorption occurs. Above a critical concentration, these electrostatic repulsions are screene, and adsorption is promoted by non-electrostatic forces, which was referred to as "screening enhanced adsorption" by van de Steeg[81].

2.5.1. Ions at the interface

When a charged surface is placed in an aqueous electrolyte solution, ions with opposite charges are attracted towards the surface. As a result, the charge distribution close to the surface is no longer homogeneous. The electrical double-layer model is a generally accepted view of charges at the interface in an electrolyte solution. There are several theories on the electrical double-layer with small differences. The Helmholtz double-layer model is the simplest representation of the double layer. It considers that the ions are tightly adsorbed on the surface in a single layer[82]. The Helmholtz model neglects the repulsion between the charges at the interface. Later Gouy and Chapman extended the Helmholtz model by introducing the diffuse layer, by using the Poisson-Boltzmann equation to describe the distribution of ions from the interface[83]. In the Gouy-Chapman model, water is a dielectric continuum and ions were considered as point charges that could approach the surface in infinitesimally short distances[84,85]. This assumption is not true due to the presence of a hydration shell around the ions. Later, Stern updated the Gouy-Chapman model by combining the Helmholtz and Gouy-Chapman models together[86]. He suggested that some ions would adhere to the surface, making the Stern layer, whereas others would form the diffuse layer, see Figure 3. This model was then referred to as the Gouy-Chapman-Stern model.

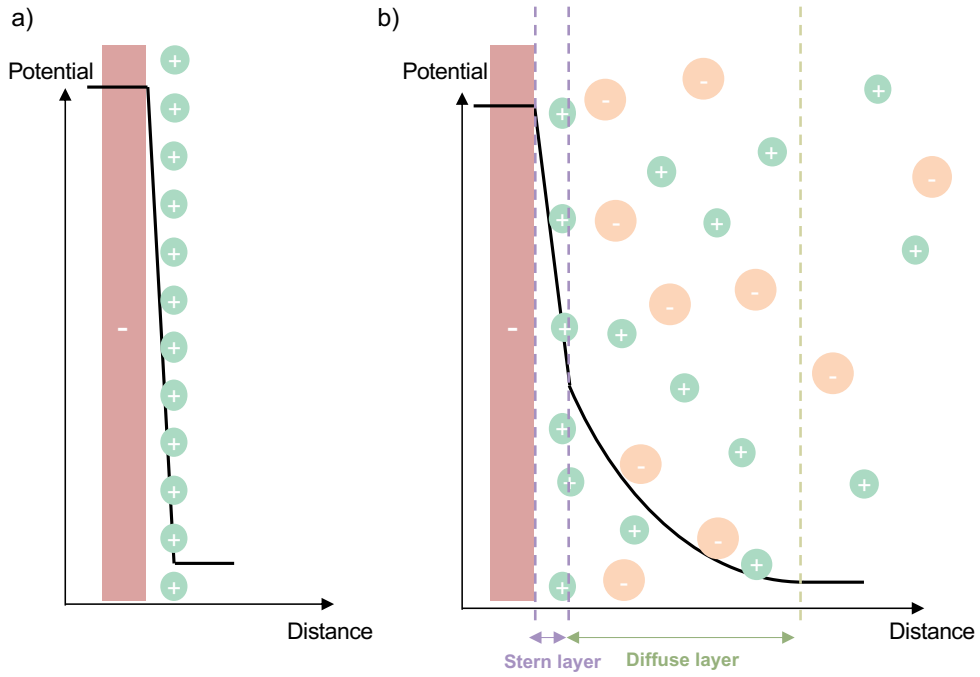

Figure 3 Illustrations of electrical double-layer models: a) Helmholtz double-layer model; b) Gouy-Chapman-Stern double-layer model.

2.5.2. Specific ion effects

Some features of ions in solution cannot be described by the classical electrolyte theories, such as the double-layer theory or the Derjaguin–Landau–Verwey–Overbeek (DLVO) theory[87]. These features are referred to as specific ion effects, where the presence of specific ions in a solution can have a significant impact on the behavior of the solution. The shortcomings of the classical theories come from the fact that they consider water (or the solvent) as a continuum and ions as charged points[84,85]. At high concentrations, this assumption is no longer justified, as the distances between ions can be as short as a couple of water molecules, which is the range of electrostatic interaction between two particles. In other words, water molecules in the hydration shells of the ions are shared, forming an interconnected matrix[88]. Furthermore, according to Debye-Hückel theory, the only interaction between ions is electrostatic, therefore, ions with similar charge and size should behave similarly. However, there are many studies in the literature that do not verify this assumption[89–93].

Franz Hofmeister was one of the first people who suggested specific ion effects and he systematically studied specific ion effects in protein precipitation with different salts[94,95]. He arranged the studied salts in the order of their precipitation power, irrespective of the proteins. Later on, this order was known as the Hofmeister series. Figure 4 shows the Hofmeister series as it is presented. In the Hofmeister series, ions are divided into two categories depending on their interactions with water. The group of ions that bring order (kosmos) to water structure are good at salting out and "stealing" the water molecules from the solute and are referred to as kosmotropes, such as sulfate or fluoride ions[96]. In contrast, the ions that do not have strong interactions with water are the structure breakers and are referred to as chaotropes. While this view of ions seems appealing due to its simplicity, new experimental studies and simulations have shown that ions cannot alter the bulk structure of water[88]. Nevertheless, the names kosmotrope and chaotrope have remained and are commonly used in the literature[97]. Currently, there is no unifying theory that can explain specific ion effects perfectly. However, in the next section, we will review some of the proposed approaches.

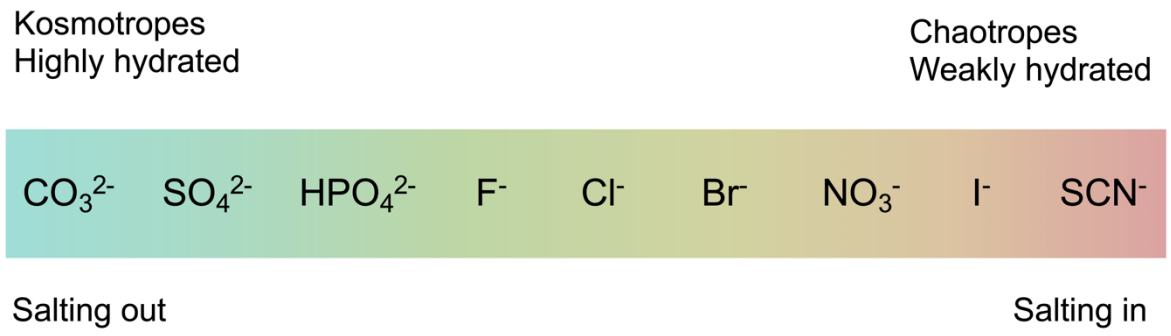

Figure 4 Hofmeister series of anions, from left to right the hydration of ions decreases.

2.5.3. The law of matching water affinity (LMWA)

The law of matching water affinity (LMWA) has greatly helped the understanding of specific ion effects. This law was developed by Collins, and it starts with the traditional classifications of ions into kosmotropes and chaotropes[97,98]. These terms, however, no longer refer to the alteration of water structure by ions, instead

they are used to describe the degree of hydration of ions where highly hydrated ions are the kosmotropes and the weakly hydrated ones are known as the chaotropes. The LMWA states that two ions of opposite charge will form contact ion pairs if they have matching water affinities. Water affinity depends strongly on the size of the ions, therefore small ions of opposite charges form contact ion pairs due to the electrostatic attraction. Large ions of opposite charges would form a contact ion pair because it would release the weakly interacting water molecules into the bulk water, where it can interact strongly with other water molecules (see Figure 5)[97,99].

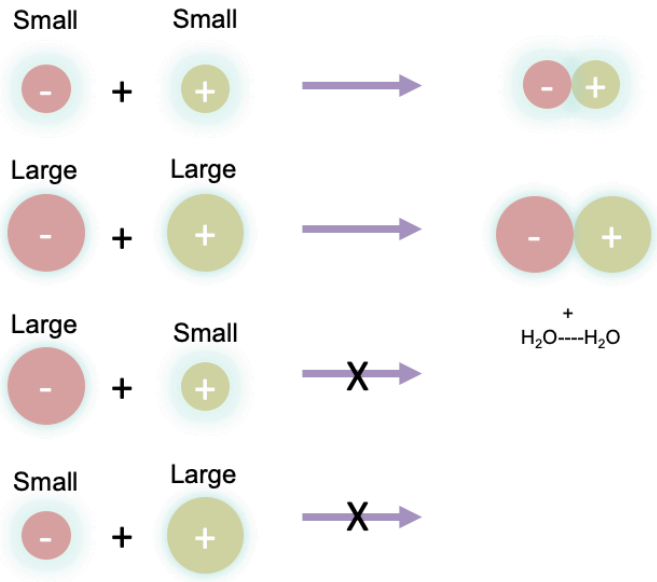

Figure 5 The LMWA. As the ion's charge density governs its water affinity, the size of the ion regulates the likelihood for oppositely charged ions to establish inner sphere ion pairs. Small ions with opposite charges readily form inner sphere ion pairs in aqueous solutions, as do large ions with opposite charges. On the other hand, oppositely charged ions with mismatched sizes do not spontaneously create inner sphere ion pairs in aqueous solutions.

2.5.4. Dispersion forces

The Derjaguin–Landau–Verwey–Overbeek (DLVO) theory effectively explains interactions within a solution under low salt concentrations, mainly when electrostatic forces dominate. However, its validity diminishes as the salt

concentration rises, typically beyond 0.1 M, where electrostatic interactions can be screened, and specific ion interactions become more prominent. To address this issue, Ninham and colleagues integrated a dispersion potential into the DLVO theory[100,101]. They showed that, by including the quantum mechanical nonelectrostatic dispersion interactions, the specific ion effects at interfaces predicted by the Lifshitz theory can be accounted for[102]. The dispersion forces were shown to account for counterion condensation on polyelectrolytes[103], specific ion effects in pH measurements[104,105], as well as surface tension in electrolytes[106].

Chapter 3: Experimental Procedures

In this chapter, an overview of the core experimental procedures that were used in this thesis is provided. First, the diffusion experiments are described, which are the heart of the studies in Paper 1, Paper 2, and Paper 3. The following section covers the principles and procedures of the adsorption studies conducted using a QCM-D, presented in Paper 3. Lastly, a full description of the methods developed by the author for the investigation of the rate-limiting step in lignin extraction through the ionoSolv process and IL impregnation studies (Paper 4) is provided. The KL used in the thesis was subjected to various characterization methods such as UV/Vis, NMR (Nuclear Magnetic Resonance), and SEC (Size Exclusion Chromatography). Detailed description of these methods can be found in the appended papers.

3.1. Diffusion experiments

The mass transport experiments were performed by utilizing tailor-made polytetrafluoroethylene (Teflon™) diffusion cells, comprising two half-cells, with RC membranes of varying pore sizes positioned between them. The pore sizes of the membranes were 3.5, 15, and 25 kDa molecular weight cut-off (MWCO) for small pore membranes (RC3.5, RC15, and RC25, respectively) and 100 and 200 nm nominal pore size for large pore membranes (RC100 and RC200, respectively). To ensure a leak-proof setup, the half-cells were tightly secured together using rods. NaOH solutions containing lignin served as donor solutions, while blank NaOH solutions of the same concentration acted as acceptor solutions. Both donor and acceptor solutions were simultaneously introduced into the diffusion cells, which were placed on an orbital shaker set at 100 rpm throughout the experiment. The orbital shaker's agitation of the donor and acceptor solutions minimized the impact of mass transport between the bulk liquid and the membrane surface. Every 24 hours, 1 mL samples from the acceptor side were withdrawn for analysis

with the UV/Vis spectrophotometer. Further details regarding the diffusion cell methodology and membranes can be found in Papers 1 and 2. The effect of the pore sizes on the diffusion of KL molecules was studied in Paper 1, the effects of solution alkalinity and lignin average molecular weight (MW) on diffusion were studied in Paper 2, and specific ion effects on mass transport were studied in Paper 3. See Table 1 for details.

Table 1 Summary of the studies presented in Paper 1, Paper 2, and Paper 3.

	Paper 1	Paper 2	Paper 3
Purpose	Study the effect of pore size on mass transport	Study the effects of solution alkalinity and lignin molecular weight on mass transport	Study specific ion effects on mass transport
RC membranes	3.5, 15, and 25 kDa MWCO (RC3.5, RC15, and RC25, respectively) and 100 and 200 nm nominal pore size (RC100 and RC200, respectively)	50 kDa MWCO	50 kDa MWCO
KL fraction	Unfractionated (KL)	Unfractionated (KL) and fractionated (KL 1-5)	Unfractionated (KL)
Alkalinity	0.1 M NaOH	0.01 M, 0.1 M, and 1 M NaOH	0.1 M NaOH
Salts	-	-	0.1 – 0.9 M NaCl 0.1 – 0.9 M $NaNO_3$ 0.05 – 0.45 M Na_2SO_4

3.1.1. Calculations for measurements of apparent diffusivity of water and lignin through the membranes

The study involved investigating the apparent diffusivity of water and lignin through membranes using the diffusion cell methodology. The experimental setup consisted of tailor-made polytetrafluoroethylene (Teflon™) diffusion cells with RC membranes placed between the cell compartments. A schematic representation of the diffusion cells is presented in Figure 6. Tritium-labeled water or lignin solutions were added to the donor side based on the specific measurement being conducted. At regular intervals, samples were withdrawn from the acceptor side, and the concentration of the diffusing species (T_2O or lignin) in these samples was measured either by a scintillation analyzer or UV/Vis spectroscopy.

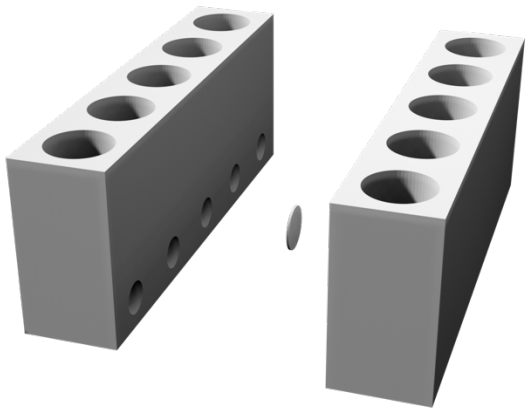

Figure 6 Schematic representation of diffusion cells, showing the two half-cells, each containing 5 samples and the holes between the half-cells where the cellulose membrane is placed.

The apparent diffusivity (D, m^2/s) of water or lignin through the membranes was calculated from the increase in concentration of the diffusing species in the acceptor chamber, following a method previously proposed by van den Mooter et al.[107] and other researchers[108,109]. According to Fick's law, the transfer rate of a diffusing substance through the membrane can be determined by the following equation:

$$\frac{dM}{dt} = -DS\left(\frac{dC}{dx}\right) \qquad \text{Equation (1)}$$

where dM/dt (g s^{-1}) represents the mass transport rate, D is the apparent diffusion coefficient, S is the membrane surface area for diffusion (m^2), and dC/dx is the concentration gradient across the membrane. By assuming a linear concentration profile through the membrane, the concentration gradient through the membrane can be written as the difference in concentration between the donor side of the membrane C_{m0} (g. m^{-3}) and the acceptor side of the membrane C_{mh} (g. m^{-3}) divided by the thickness of the membrane h (m). By inserting this in Equation 1, Equation 2 results as follows:

$$\frac{dM}{dt} = DS\left(\frac{C_{m0} - C_{mh}}{h}\right) \qquad \text{Equation (2)}$$

It is assumed that the presence of an aqueous boundary layer on either side of the membrane does not have a significant impact on mass transport through the membrane. To establish a relationship between the bulk concentrations in the donor and acceptor chambers and the concentrations at the membrane, the partition coefficient K is defined as:

$$K = \frac{C_{m0}}{C_d} = \frac{C_{mh}}{C_a} \qquad \text{Equation (3)}$$

where C_a and C_d represent the concentrations of the diffusing substance in the bulk of the acceptor and donor chambers, respectively. It is assumed that the agitation of the solutions in the diffusion cells is sufficiently high to create homogeneous solutions, thereby neglecting any mass transport resistance between the bulk and the membrane surface. Consequently, the concentration of lignin in the bulk and at the membrane boundaries is considered to be the same. Therefore, the partition coefficient is considered to be equal to 1. The mass of the diffusing substance in the donor and acceptor chambers at time t = 0 s are represented as M_d and M_a (g), respectively, consequently, the concentrations in the donor and acceptor chambers can be calculated as:

$$C_d = \frac{(M_d - M)}{V}$$ Equation (4)

$$C_a = \frac{(M_a + M)}{V}$$ Equation (5)

Here, M (g) represents the mass change resulting from diffusion and V (m^3) denotes the volume of the solution in the chambers. Given that at t = 0, there are no diffused substances in the acceptor chamber (M_a = 0), Equation 2 can be reformulated as Equation 6:

$$\frac{dM}{dt} = \frac{DKS}{h}\left(\frac{M_d - M}{V} - \frac{M}{V}\right)$$ Equation (6)

Equation 7 can be obtained by integrating Equation 6 (K =1 due to high agitation of solution):

$$\frac{2DS}{hV}t = -ln\left(\frac{M_d - 2M}{M_d}\right)$$ Equation (7)

Assuming that the reduction in lignin concentration in the donor chamber is negligible, we can calculate the apparent diffusivity using Equation 8:

$$\frac{2DS}{hV}t = -ln\left(\frac{C_0 - 2C_a}{C_0}\right)$$ Equation (8)

The concentration C_0 and C_a (g m^{-3}) correspond to the donor solution at the start and the acceptor solution at time t, respectively. Given the assumption of a negligible decrease in lignin concentration in the donor chamber, the driving force remains constant. Thus, Equation 9 can be applied as long as this assumption holds, which is primarily at the beginning of the experiments.

The diffusivity of lignin or water through the membranes was calculated by plotting the right side of Equation 8 against time. C_a was determined at various time points by analyzing the concentration of the diffusing substance in the samples collected from the acceptor chamber.

3.2. Adsorption studies using QCM-D

In this thesis, the adsorption of lignin molecules in the presence of various ions was studied using the QCM-D method. QCM-D is an acoustic approach that determines the aerial mass of the adsorbed polymer layer and any associated solvent. A detailed description of the QCM-D method can be found in Paper 3.

QCM-D's fundamental element consists of a piezoelectric quartz crystal sensor coated with either gold or silica, as illustrated in Figure 7. When an oscillating electric field is applied across the quartz crystal, it triggers vibrations at its resonance frequency. The frequency of these vibrations is directly linked to the mass present on the crystal's surface. Consequently, during adsorption events, the frequency change can be converted into the adsorbed mass using the Sauerbrey relation:

$$\Delta m = -\left(\frac{C_{QCM}}{n}\right) \Delta f \qquad \text{Equation (9)}$$

where Δm is the mass change, C_{QCM} is the mass sensitivity constant (C_{QCM}= 17.7 ng cm^2 Hz^{-1} at f = 5 MHz), n is the overtone number, and Δf is the frequency change.

Usually, when hydrophilic polymers and biomacromolecules are adsorbed, the resulting layers are not rigid and have a significant viscous component. This causes rapid energy dissipation, reducing the crystal's resonance frequency response, as depicted in Figure 7. QCM instruments use this energy dissipation to provide valuable information about the viscoelastic characteristics of the adsorbed layer as the dissipation factor D_n:

$$D_n = \frac{1}{\pi f_n \tau} \qquad \text{Equation (10)}$$

The parameter τ represents the rate at which the amplitude decreases when the driving AC voltage is turned off.

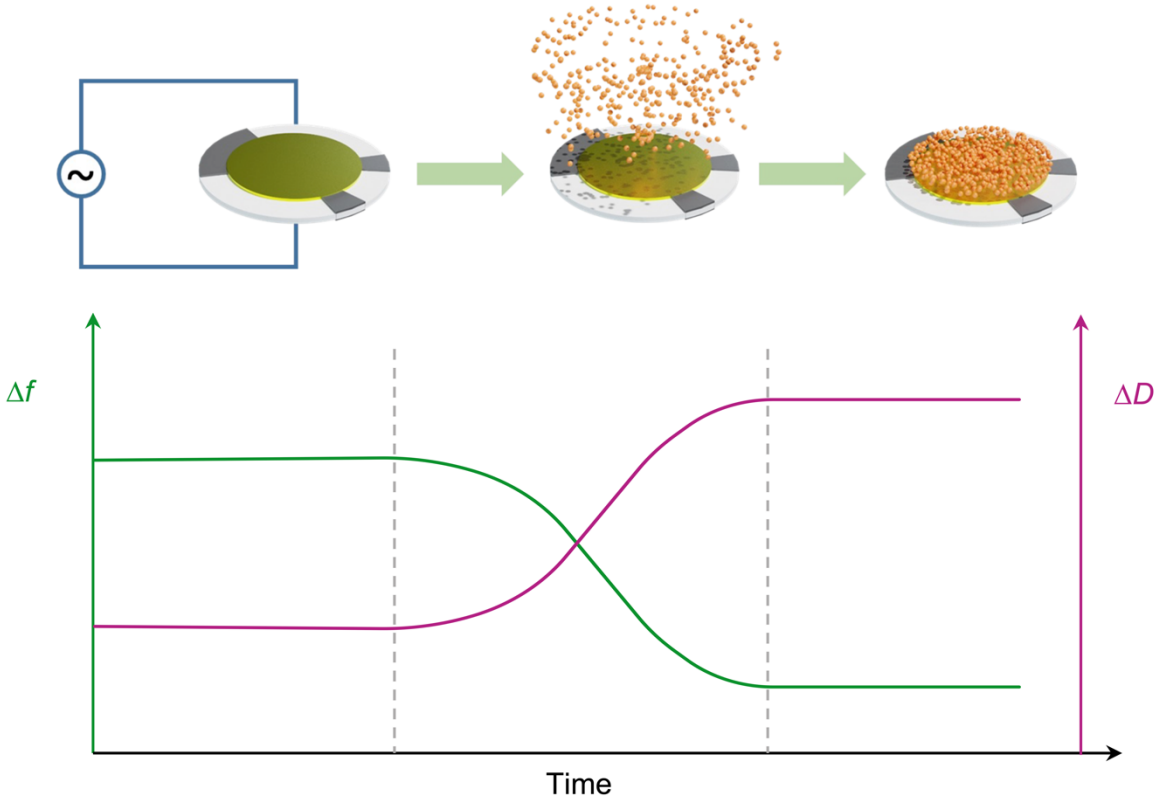

Figure 7 An illustration representing a QCM-D sensor at different stages of adsorption (top) and the corresponding changes in dissipation and frequency (bottom).

When polyelectrolytes are adsorbed on cellulose surfaces, the resulting adsorbed layers commonly exhibit viscoelastic behavior[110,111]. Therefore, it is crucial to consider the viscoelastic nature of the adsorbed layer when calculating the adsorbed mass. The Sauerbrey equation does not account for viscoelasticity. However, it is used for estimation and convenience[112]. To account for the viscoelastic nature of the adsorbed layer, Johannsmann's model can be used. The simplified form of Johannsmann's model can be seen in Equation 11.

$$m^* = m^o\left(1 + \hat{\jmath}(f)\frac{f^2 d^2 \rho}{3}\right) \qquad \text{Equation (11)}$$

where m^0 is the true sensed mass, m^* is the equivalent mass, $\hat{J}(f)$ is the complex shear compliance, ρ is the density of the fluid, d is the thickness of the film, and f is the resonance frequency.

The assumption is that $\hat{J}(f)$ remains constant regardless of the frequency within the accessible range. The true sensed mass m^0 is determined graphically by plotting the equivalent mass against the square of the resonance frequency (f^2). Note that when using Johannsmann's model, the measured mass includes both the dry mass of the adsorbed polymer and the mass of water associated with the adsorbed layer. Therefore, the true sensed mass is not equivalent to the dry mass of the adsorbed polymer. In this thesis, the adsorption of dissolved KL molecules in the presence of various salts (NaCl, $NaNO_3$, and Na_2SO_4) on an RC surface was studied.

The RC surfaces were prepared on gold QCM-D surfaces for adsorption studies. In short, trimethylsilyl cellulose (TMSC) was dissolved in toluene (10 wt%) and centrifuged at 5000 rpm for 15 minutes and then the supernatant was separated and used for spin coating (see Figure 8). After the surfaces were coated, they were exposed to HCl vapour for 30 minutes. The regeneration of surfaces was confirmed by recording a Fourier-transformed infrared spectrum of the surfaces, where distinct Si-C characteristic peaks at 848 and 1253 cm^{-1} would vanish after the cellulose's regeneration[113]. The surface morphology of the RC film was characterized by atomic force microscopy (AFM). The root-mean-square roughness value, computed from AFM images, was 0.94, suggesting a relatively flat surface similar to previous literature reports[113].

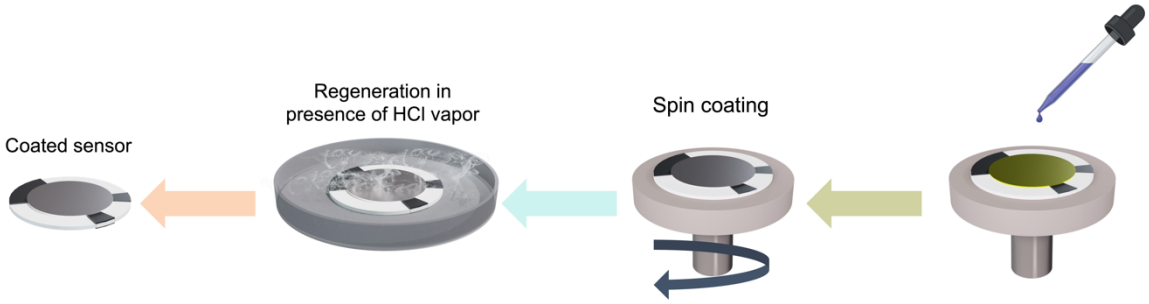

Figure 8 An illustration depicting the procedure of applying RC onto QCM-D sensors: Initially, an 80 µl TMSC solution in toluene was spin-coated onto the sensor's surface, followed by placing the sensor alongside a 2 ml solution of 10% HCl in a petri dish with a closed lid.

3.3. Investigation of the rate-limiting step in the extraction of lignin through ionoSolv pretreatment

The ionoSolv method for wood fractionation involves a series of crucial steps for the wood to start reacting with ILs. Firstly, impregnation allows the IL to penetrate the wood's porous structure. Mass transport is vital in this step for transporting ions to reaction sites by diffusing the IL from the wood's surface to its inner regions, where the reactive sites are present. Once the IL reaches these sites, it is ready to start delignification reactions that require high temperatures. Consequently, by raising the temperature, lignin is degraded and solubilized. After solubilization, the products must diffuse out of the wood structure into the bulk IL , leaving behind a cellulose-rich pulp. Understanding and optimizing these steps are crucial for enhancing the efficiency of lignin extraction and wood fractionation through the ionoSolv method. Each of these steps can potentially be the rate-limiting step. The following experiments were designed to identify which step is the rate-limiting step.

Three types of wood samples were prepared, namely, *dry, impregnated,* and *impregnated-reacted*. All samples were chopped into approximately 1 x 1 x 2 cm (R x T x L) dimensions from the sapwood of a Norway spruce (softwood). The samples were all first air dried, then dried in an oven at 80 °C for 1 hour, followed by exposure to vacuum for another hour.

The *dry* samples were the wood pieces that were kept fully dry until the start of the experiments. The *impregnated* samples were prepared by soaking the prepared wood pieces in the chosen protic IL ([DMBA][HSO_4]) first under vacuum for 6 hours, followed by soaking in ambient air until fully saturated with the IL. To ensure full impregnation of the wood pieces, their weight change was monitored over time and, when the weight stabilized, they were considered fully impregnated. The wood samples used here (considering their size and the species) can take up to 2 times their weight in the IL (DMBA][HSO_4]) over at least three days of soaking. The *impregnated* samples were one step ahead of the *dry* samples, meaning that as soon as the temperature was raised, the delignification started, since the chemicals were already at the reaction sites. The last type of sample was the *impregnated-reacted* sample. To prepare these samples, the already impregnated samples were placed in the oven at 150 °C for 45 minutes. These samples were already two steps ahead of the *dry* samples since the IL was inside the wood pieces and delignification was partially complete. Hence, some degraded lignin molecules were now available in the structure. Therefore, as soon as the samples came in contact with the IL, lignin began diffusing out of the structure.

To ensure a one-directional diffusion, the wood pieces were covered from all sides except one by embedding the pieces in a silicon resin. In this way, the pieces could later be examined to observe how their structure had been damaged, where they were in direct contact with the bulk IL, and where they were not. Also, in the *dry* sample, it could be observed how homogeneously the reactions occurred and whether the IL had reached the bottom of the wood piece during the time the reactions were occurring. As described, after embedding the samples in silicon, all sides were covered except one (the top side), see Figure 9. Next, IL containing 20% water with a ratio of wood to IL of 1:5 was poured on the samples and they were placed in an oven at 150 °C with tightly closed caps. At specific time intervals, the samples were removed from the oven, corrected for the lost water, and a 100 µL sample from the outer liquid was taken. The collected samples were then diluted

and their UV/Vis spectra were recorded. The concentration of lignin was then quantified using the 280 nm peak and a previously constructed standard curve.

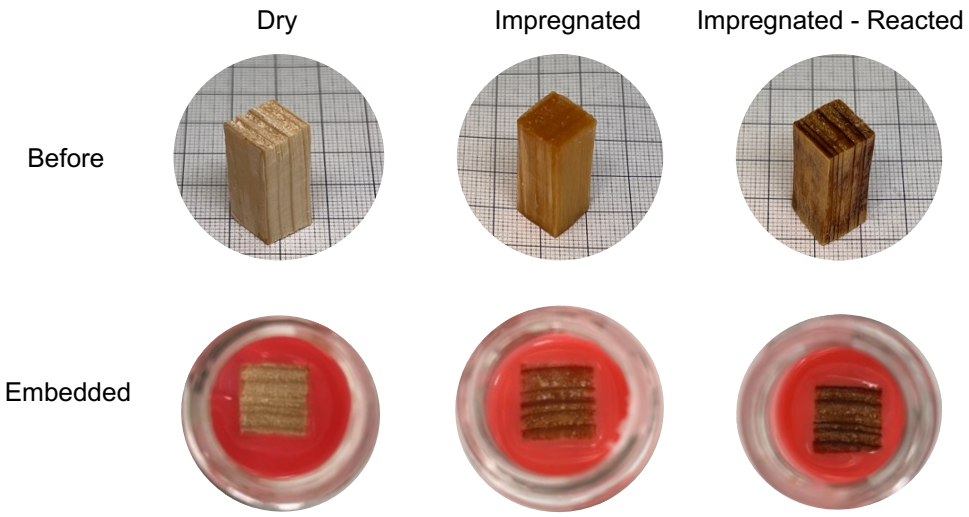

Figure 9 Photographs of the samples prior to the start of the experiments.

3.3.1. Investigating the effect of temperature and water content on the impregnation of wood pieces with ionic liquid

Since impregnation can significantly affect the process rates, it is important to investigate influential parameters on the impregnation of wood pieces. Temperature has a significant effect on diffusion and mass transport processes, therefore, one of the parameters studied here was temperature. Another important parameter is the viscosity and surface tension of the diffusing liquid. These two parameters are greatly influenced by the water content of the IL, therefore, the other variable studied here was the water content of the liquid.

The following procedure was designed to investigate the impact of temperature, water content, and vacuum on the impregnation and mass transport of [DMBA][HSO4] into wood pieces. Dry wood pieces measuring 1 x 1 x 3 cm (R x T x L) were chopped from the sapwood of a spruce tree. The samples were first air dried at room temperature for at least four months, then, prior to the experiment, they were dried in an oven at 80 °C for an hour and placed under vacuum for another hour. The prepared samples were then placed in a 100 mL glass pressure

tube. [DMBA][HSO_4] containing either 20% or 50% water content was then poured over the wood pieces at a wood-to-IL ratio of 1:10. The pressure tube was securely sealed to prevent any water loss and placed in an oven at the desired temperatures (90, 120, or 150 °C) or subjected to vacuum at room temperature. After 30 minutes, the wood pieces were removed from the liquid, gently patted with a paper towel to remove excess liquid from the surfaces, and their weights were recorded.

Chapter 4: Summary of the Key Findings

This chapter aims to provide a summary of the key findings of the appended research papers. Section 4.1 and the subsections focus on finding the influential parameters affecting the mass transport of KL molecules from cellulose confinements. The following parameters were investigated in this section: Size of the confinement (Paper 1), alkalinity and MW of lignin (Paper 2), and specific ion effects and the presence of salts in the solution (Paper 3). Section 4.2 is dedicated to the study of the mass transport of ILs into the wood structure and investigating the rate-limiting step in the ionoSolv process (Paper 4).

4.1. Important parameters affecting mass transport of lignin through confinements

The mass transport of lignin through confined spaces is influenced by several key parameters that collectively impact the efficiency of the process. The size of the confinements plays an important role, affecting the accessibility and availability of the space lignin moves through. This was studied in Paper 1 using the diffusion cell setup and RC membranes with a variety of pore sizes (ranging from 200 nm to a few nm), as explained in the experimental methods chapter. Alkalinity is another critical factor influencing the association and interactions between lignin molecules and the confining surfaces, which, in turn, influence the rate of mass transport. Additionally, the MW of lignin contributes significantly to its diffusion behavior, with smaller molecules tending to diffuse more rapidly. These two parameters were studied in Paper 2, using the same methodology. To study the effect of the MW of lignin, a solvent fractionation[114] step was performed on the KL prior to the experiments. The presence of salts further complicates the mass transport process, as they can alter lignin's interactions with the cellulose surface or the behavior of lignin in the solution. The same diffusion cell methodology combined with QCM-D measurements was used to study the mass transport and adsorption of lignin in the presence of salts.

4.1.1. Pore sizes

In the pulping process, the diffusion of released lignin molecules predominantly takes place within the fiber cell wall, lumen, and pits. Pits, serving as channels connecting adjacent lumens in the wood structure, facilitate communication between the lumens. These pits possess a membrane containing nanoscale pores[70]. The wood cell wall consists of bundles of cellulose immersed within a matrix of lignin and hemicelluloses. These cellulose bundles, with diameters of 20-25 nm, are spaced apart on the nanometer scale[115]. The pores found in membranes like RC3.5, RC15, and RC25 (MWCO of 3.5, 15, and 25 kDa, respectively) approximate the dimensions of the distances between the bundles of microfibrils in the secondary cell wall[116]. When lignin is liberated and solubilized in the solution, it migrates from the fiber wall into the lumen, subsequently moving into the bulk liquor via either the larger pits present in the cell wall or through the lumen or the open lumen ends. Notably, some of the pit membranes dissolve during the pulping process, given their elevated hemicellulose content. These larger confinements are exemplified by the membranes possessing larger pores, such as RC100 and RC200 (with nominal pore sizes of 100 and 200 nm, respectively).

Figure 10 shows the concentration increase in the acceptor chamber of diffusion cells, where lignin molecules passed through the membrane from the donor chamber. The curves show a linear trend in the concentration increase over time, indicating that the diffusion proceeded with a steady trend. As expected, the diffusion rate through the membrane was larger for large pore membranes than the small pore membranes. The lower diffusion rate through the small pore membrane can be attributed to the fact that large lignin molecules or lignin clusters could not pass through these pores, whereas, for RC100 and RC200 membranes, the size of the pores compared to the size of lignin molecules is large enough to allow all molecules, regardless of whether they are in a cluster or not, to pass through the membrane.

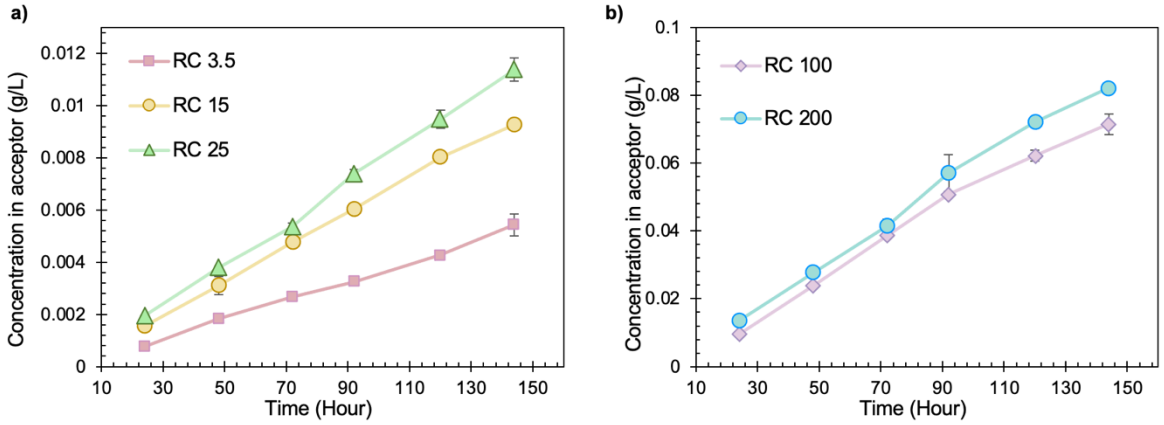

Figure 10 Concentration of lignin in the acceptor chamber of the diffusion cells with respect to time: a) Small pore membranes (RC3.5, RC15, and RC25); b) Large pore membranes (RC100 and RC200).

To investigate the molecular weight of the molecules that passed the membrane, SEC was used. The SEC chromatographs and experimental details can be found in Paper 1. The average molecular weights of the KL used in the donor solution and the lignin molecules transported to the acceptor are summarized in Table 2. It is important to note that these absolute MW values were determined using polyethylene glycol standards, which may not reflect the characteristics of lignin molecules. Hence, it is advisable to employ these values solely for the purpose of comparison. Nevertheless, there was a significant difference between the size of the molecules found on the acceptor side of the small pore membranes compared to the acceptor side of large pore membranes. While the MWCO of small pore membranes were equal to or larger than the KL, a significant amount of them could not pass through the membrane within the time span of the experiments. This observation suggests that the molecules either interacted in clusters or that the diffusion of larger molecules through the pores was exceptionally slow.

Table 2 The average molecular weights of KL species that diffused from the donor side through the membranes to the acceptor side.

	Acceptor RC3.5	Acceptor RC15	Acceptor RC25	Acceptor RC100	Acceptor RC200	Donor KL in 0.1M NaOH
MW (kDa)	0.9	1.2	1.5	3.1	3.1	3.9
Polydispersity index	1.7	1.8	2.2	2.8	2.8	2.8

UV/Vis absorbance spectra were utilized to study the chemical variations between lignin molecules from the initial donor samples and those transported through the membrane into the acceptor chamber. The spectra of acceptor samples derived from RC100 and RC200 membranes closely resemble the spectrum of the donor sample, however, they exhibited an elevated absorbance around 350 nm compared to the donor spectrum, see Figure 11.

In contrast, the acceptor spectra corresponding to the RC3.5, RC15, and RC25 membranes differed from the original lignin in the donor chamber. One of the observed differences was that, at wavelengths around 425 nm, the donor spectrum and the acceptor samples from RC100 and RC200 membranes exhibited a greater absorbance compared to the acceptor spectra for the small pore membranes (as indicated by the green arrow in Figure 11a). This higher absorbance could be from scattering induced by larger molecules and/or small, loosely aggregated clusters of lignin molecules that were only able to pass the large pores. These dispersed clusters could be formed through interactions among lignin molecules. These experiments were performed in 0.1 M NaOH and, at such high alkalinity, the presence of lignin clusters or associations is not very common. However, as documented by Rudatin et al., it is possible[117]. They suggested that the extent of

association in small and large lignin molecules is different. The higher the MW of the molecules, the more association they show at high alkalinities. The role of MW and alkalinity will be discussed in further detail in the next section.

The more notable distinction between the spectra of the acceptor solutions is seen in the spectra of the lignin that has passed the small pore membranes, where an additional peak at 350 nm was observed. This peak could not be seen in the acceptor spectra of large pore membranes. It has been reported in the literature that phenolic lignin units conjugated in the α-position would show a maximum in the absorbance spectrum at around 350 nm when dissolved in an alkaline solution[118,119]. If the pH of the solution is reduced to neutral conditions, the maximum at 350 nm disappears and only one maximum at 280-300 nm remains. Simultaneously, a peak around 300 nm under alkaline conditions indicates the presence of unconjugated phenolic lignin components. This peak shifts to 280 nm when the pH is lowered to neutral conditions[120–122].

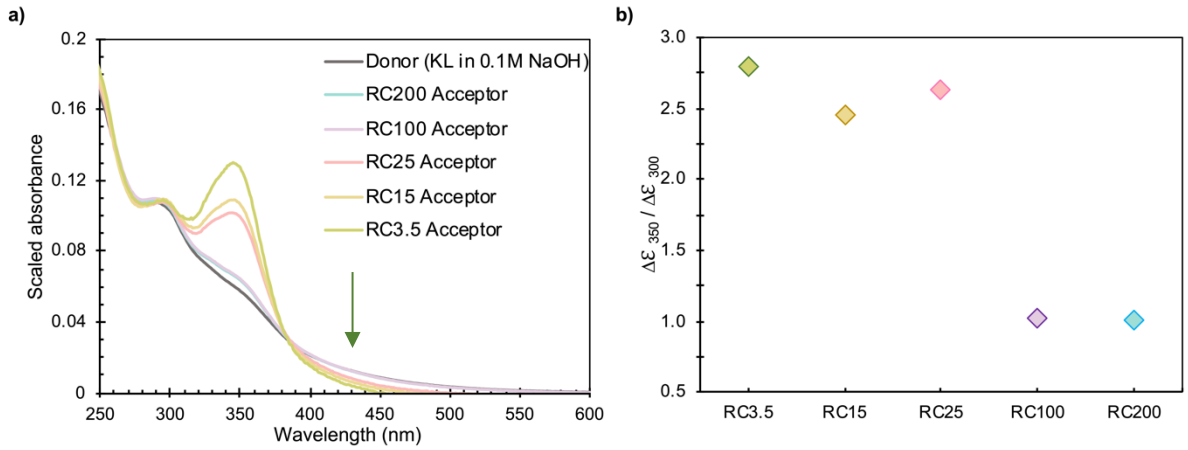

Figure 11 a) UV/Vis spectra, scaled for comparison, obtained from samples collected at the acceptor side of diffusion cells after 168 hours; b) Ratio of ionization difference (Δε) at 350 nm to 300 nm, which corresponds to the relative concentration of conjugated to unconjugated units.

Zakis et al. (1995) and Gärtner et al. (1994) introduced a method to compare the quantities of conjugated and unconjugated lignin compounds, such as carbonyl- or double-bond conjugated phenols like stilbenes and quinones[118,119]. This method

was applied to the various acceptor samples in this study. By subtracting the absorbance spectra obtained under alkaline and neutral conditions, they calculated Δε (see Paper 1). While this method may slightly underestimate the available phenolic hydroxyl content in KL samples, it is valuable for making comparisons[122,123]. Figure 11b demonstrates Δε at 350 nm relative to Δε at 300 nm. This correlation reflects the linear relationship between the ratio of conjugated phenols to unconjugated phenols[118,119].

The RC3.5, RC15, and RC25 samples exhibited a higher $\Delta\varepsilon_{350}/\Delta\varepsilon_{280}$ compared to the RC100 and RC200 samples. This indicates that a greater proportion of conjugated phenolic structures relative to unconjugated ones has been transported to the acceptor side through the membranes with smaller pore sizes, which confirms a chemical fractionation between the donor and acceptor of small pore membranes.

The presence of more conjugated structures in the acceptor solutions could be a result of size fractionation. As presented earlier, a clear size fractionation exists between the donor and acceptor of small pore membranes. Transported molecules may consist of smaller lignin fragments, such as monomers and oligomers, which are primarily generated during the kraft process when aryl-ether bonds are cleaved. When these bonds are broken, intermediates such as quinone methide are formed, leading to the formation of conjugated bonds on α or ß carbons and, therefore, conjugated phenolic end groups are produced.

Furthermore, the size and shape of the molecule can affect its transport through confinements. Polymers, regardless of their linear, branched, or closed circular structure, can navigate through narrow channels using a mechanism called reptation[124]. In the reptation theory, chains do not move as a whole, but rather segments of the molecule move through constraints, creating a motion similar to snakes moving through tall grass[125]. Such a mechanism can allow the large lignin molecules to pass through the small pores of RC3.5, RC15, and RC25, even if it necessitates that the lignin molecules should possess sufficient flexibility to adopt

various configurations. In large pore membranes, the large lignin molecules do not need to rearrange themselves to pass through the pores. Figure 12 provides the schematic summary of lignin molecules passing through large and small pores.

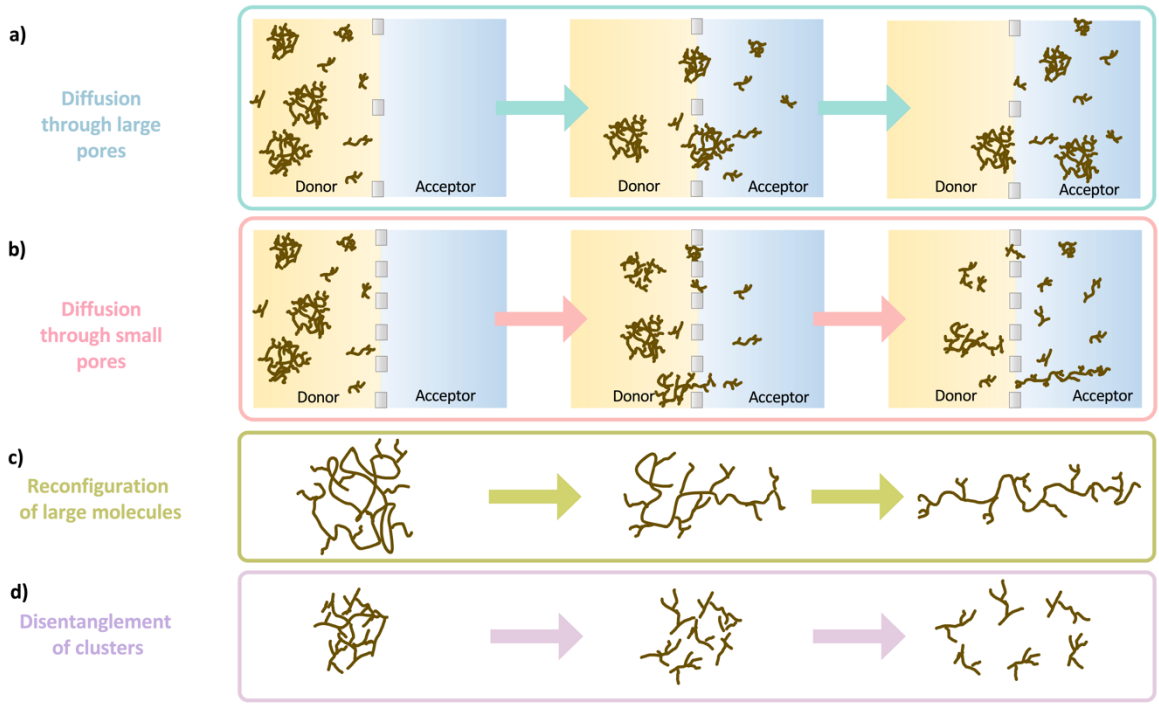

Figure 12 a and b) The diffusion of lignin molecules through membranes in diffusion cells is illustrated in the schematic diagrams; c) the larger lignin molecules undergo reconfiguration, facilitating their movement through a membrane using a reptation-like mechanism; and d)the lignin clusters undergo disentanglement or dissociation, enabling their passage through a membrane (d).

4.1.2. Alkalinity and molecular weight

The alkalinity of the solution can influence the interactions between lignin molecules and between lignin and the membrane, as well as the structure of the membrane. The same diffusion cell methodology as before was used here and, to investigate the effect of alkalinity, three concentrations of NaOH (0.01, 0.1, and 1 M) were chosen. The KL was soluble in all these NaOH concentrations. It is known that cellulose can swell in alkaline solutions[126]. Therefore, prior to lignin diffusion experiments, a series of water diffusivity measurements were performed on the membranes to observe the changes that the alkaline solution can cause to the

membranes and how they would affect diffusivity through the membranes. Figure 13 shows the tritium-labeled water diffusivity in various alkalinities. As the alkalinity was raised, the diffusivity also increased slightly. This indicates that the properties of the membrane that affect the diffusion of molecules through it have also been altered by alkalinity, possibly due to cellulose swelling.

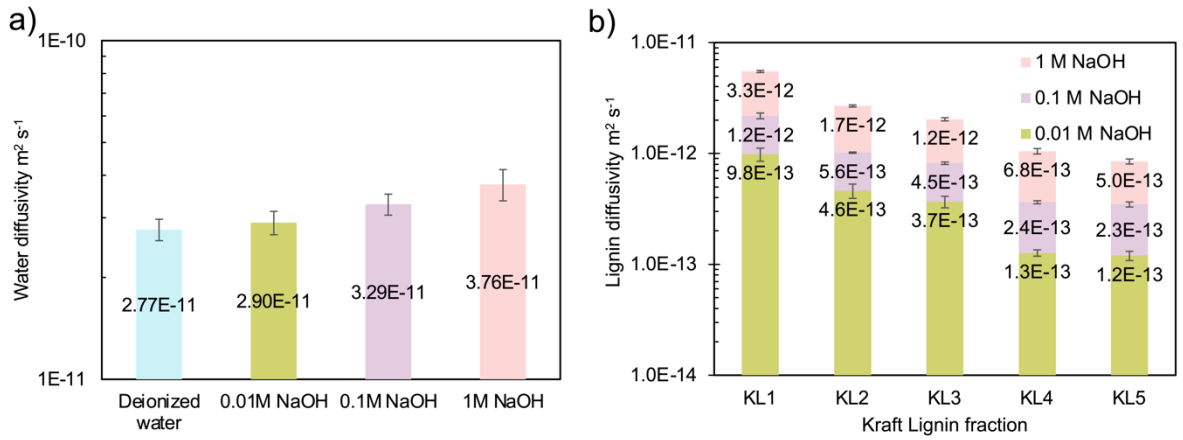

Figure 13 a) Diffusivity of tritium-labeled water through the 50 kDa MWCO membrane at various levels of alkalinity. b) Variation in diffusivity of fractionated lignin under different alkaline conditions.

The molecular weight of the diffusing species (here lignin) can significantly affect the rate of diffusion, where smaller molecules have a higher diffusion coefficient. The effect of MW of lignin was intended to be studied simultaneously to the alkalinity experiments. Hence, a solvent fractionation step was employed on the KL, which separated lignin into five fractions with increasing MW from KL1 to KL5[114]. Details on the MWs and OH^- functionalities of the fractions can be found in Paper 2.

Figure 13b shows the diffusivity of lignin fractions through the membranes at different alkalinities. As expected, the lower the MW, the higher the lignin diffusivity through the membrane. Higher alkalinity in the solution also leads to higher diffusivity, similar to the water diffusivity experiments. However, while increasing the alkalinity from 0.01 M NaOH to 1 M NaOH, the water diffusivity increased by only about 30%, whereas the lignin diffusivity increased by 3 to 5

times. This shows that the increase in membrane diffusivity due to swelling could not solely account for the increase in lignin diffusivity and higher alkalinity was also affecting lignin molecules.

Altering the alkalinity has diverse effects on lignin molecules in solution, including lowering the association between molecules. It has been shown in the literature that, by elevating the OH^- ion concentration, the association between lignin molecules is reduced[79]. This comes from lignin's elevated charge at higher alkalinity, prompting greater repulsion, thus inhibiting electrostatic association and aggregate formation. The molecules may also adhere to fully bleached softwood kraft pulp fibers, as previously suggested by Norgren and Bergfors[127]. Adsorption onto the cellulose membrane surface can decelerate their diffusion through pores. The likelihood of adsorption diminishes at higher solution alkalinity, owing to the aforementioned factors, making the adsorption process less prominent when lignin dissolves in a good solvent.

While the association of lignin molecules at high alkalinity is limited, it is still possible. In fact, Rudatin et al. [117] reported the association of large lignin molecules even at very high pH levels of 13.5. Interestingly, when the alkalinity of our solutions was increased from 0.01 M to 0.1 M NaOH, an increase in diffusivity of 1.9 for large MW fractions (KL4 and KL5) was observed, while, in the case of the lower MW fractions (KL1, KL2, and KL3) the increase in diffusivity was about 1.2. This observation can be explained by the tendency of various fractions to associate. Association between lignin molecules strongly depends on the electrostatic repulsion between molecules, therefore, the degree of ionization of the molecules can significantly alter their association behavior. The pKa of lignin's phenolic groups depends on their MW, where the higher the MW of lignin, the higher their pKa[128]. The shape of the dissociation curve for the phenolic groups also changes with the molecule's MW, with flatter curves for larger molecules. This indicates that at a certain alkalinity level, the number of deprotonated phenolic units is lower for large compared to small molecules. Therefore, by increasing alkalinity from 0.01 to 0.1 M NaOH, the increase in the number of charged molecules can

potentially be higher in high MW fractions, since the low MW fractions were already mostly charged even at lower alkalinity levels[128].

To understand the chemical differences between the lignin molecules that passed through the membrane and the donor samples, their UV/Vis absorbance spectra were compared under different alkalinities. Figure 14 shows the scaled UV/Vis absorbance spectra for KL1 and KL5 fractions from both the donor and acceptor samples taken from the diffusion cells. KL1 and KL5 showed the most noticeable differences and were, therefore, compared here. More detailed UV/Vis spectra for all fractions can be found in Paper 2. A significant difference was seen between the UV/Vis spectra of the acceptor and donor samples. There is a distinct peak around 350 nm in all acceptor samples, while the donor spectra only show a slightly higher absorption around 350 nm. This 350 nm peak was similar to what was observed in the small pore membrane acceptor samples in the previous section and Paper 1 and can be attributed to conjugated phenolic groups in the alkaline solutions[118]. Additionally, a small bump around 320 nm in the acceptor samples is also noticeable. When higher NaOH concentrations (0.1 and 1 M NaOH) were used, the peak in the donor spectra moved from 280 nm to 300 nm, which was especially noticeable in higher MW fractions like KL5. As discussed in section 4.1.1, the groups related to conjugated phenols and dissociated aromatic carboxylic acids typically absorb around 350 nm. Also, aromatic carboxylic groups and α-carbonyl groups absorb around 320 nm, which explains the bump seen at 320 nm[129].

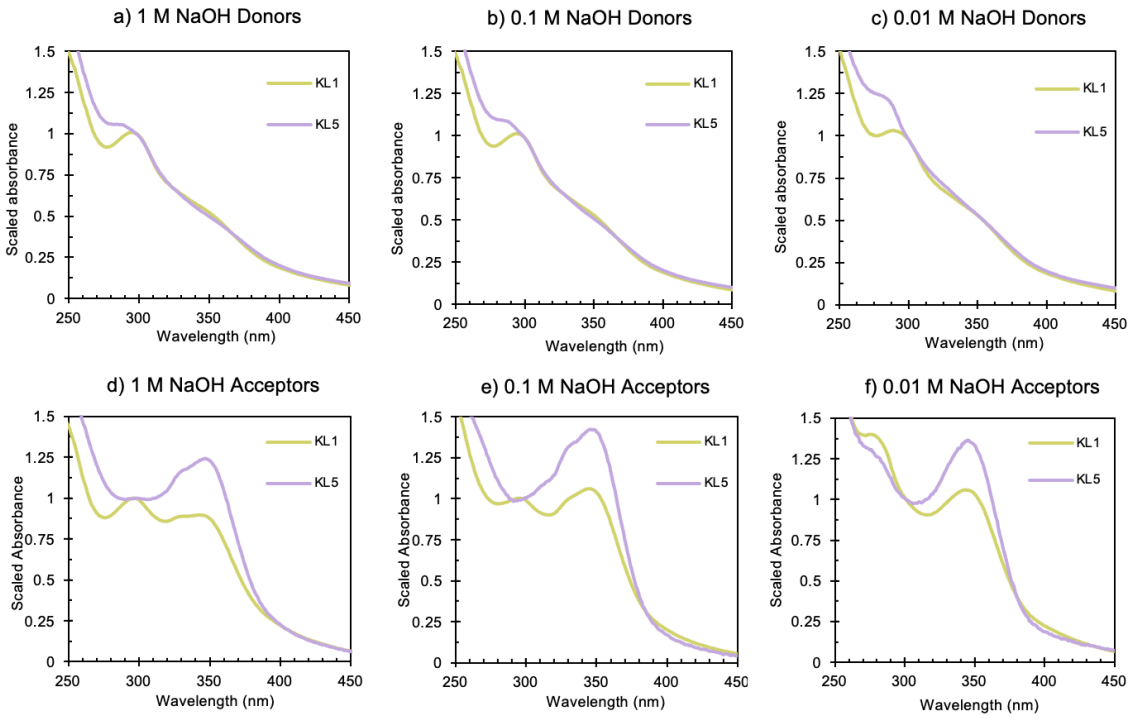

Figure 14 UV/Vis absorbance spectra of the KL1 and KL5 donors at the beginning of the experiments in a) 1 M NaOH; b) 0.1 M NaOH; c) 0.01 M NaOH and the spectra of the acceptor samples after 168 hours in d) 1 M NaOH; e) 0.1 M NaOH; f) in 0.01 M NaOH.

A similar potential explanation is that smaller lignin molecules, like monomers or oligomers, tend to have more conjugated structures. Meanwhile, small molecules have a higher diffusion coefficient, allowing them to move faster through the membrane compared to larger molecules and, therefore, they are found more than the unconjugated molecules in the acceptor solution.

4.1.3. Presence of salts in the solution

The third parameter that affects the mass transport of dissolved lignin through cellulose confinements that was studied is specific ion effects and the presence of salts in the solution.

The solubility limit of lignin, water diffusivity, and lignin diffusivity through the membranes in the salt solutions are presented in Table 3. The solubility limit of lignin drastically decreased with increasing salt concentration, especially for NaCl

and Na_2SO_4, which can be attributed to a charge screening effect. The solubility decrease was less significant in the presence of $NaNO_3$. Norgren et al. also observed that nitrate ions increased the stability of lignin molecules in solution and improved their solubility in alkaline solutions[130].

At lower salt concentrations, the solubility of lignin remained relatively consistent across all salt types, showing a slightly elevated solubility in the presence of a 0.1 M cation concentration of Na_2SO_4. However, a shift in this trend emerged when the cation concentration was elevated to 0.9 M. Notably, the solubility of lignin exhibited a reversed order, being at its lowest in the Na_2SO_4 solution while nearly tripling in the nitrate-containing solution. The reversal of the Hofmeister series at lower salt concentrations and its agreement with the direct Hofmeister series at higher concentrations has been documented in earlier literature[131].

The weakly hydrated ions, such as nitrate, tend to interact with the surface of the macromolecules and shed their hydration layer, therefore increasing the hydrophilicity of the macromolecules, which can lead to a higher solubility limit of the molecule[132,133].

Similar to the previous papers, the diffusion of lignin through cellulose membranes was studied using the diffusion cell methodology. The transport of molecules across the membrane displayed a consistently linear pattern, confirming the membrane's stability throughout the experiments (see Paper 3). As presented in Table 3, elevating the concentrations of $NaNO_3$ and NaCl resulted in an accelerated transport of lignin through the membrane. A similar effect was observed with Na_2SO_4, where an increase in salt concentration from 0.05 M to 0.2 M enhanced lignin transport. Nevertheless, when the Na_2SO_4 concentration was further elevated to 0.45 M, a slight reduction in lignin transport through the membrane was observed. This indicates the possibility of specific ion effects at higher salt concentrations, where mass transport of lignin is limited due to the aggregation of lignin molecules in the presence of sulfate ions.

Table 3 Summary of the measured solubility limit of lignin, the diffusivity of water, and the diffusivity of lignin in the solutions.

Solution	Solubility limit of lignin (mg/mL)	Water diffusivity (m^2/s)	Lignin diffusivity (m^2/s)
0.1 M NaCl + 0.1 M NaOH	54.0	4.2×10^{-11}	3.3×10^{-13}
0.4 M NaCl + 0.1 M NaOH	44.3	4.6×10^{-11}	3.6×10^{-13}
0.9 M NaCl + 0.1 M NaOH	17.4	6.8×10^{-11}	5.3×10^{-13}
0.1 M $NaNO_3$ + 0.1 M NaOH	53.6	4.9×10^{-11}	3.1×10^{-13}
0.4 M $NaNO_3$ + 0.1 M NaOH	45.6	7.0×10^{-11}	3.6×10^{-13}
0.9 M $NaNO_3$ + 0.1 M NaOH	39.2	7.5×10^{-11}	5.5×10^{-13}
0.05 M Na_2SO_4+ 0.1 M NaOH	59.5	4.2×10^{-11}	2.7×10^{-13}
0.2 M Na_2SO_4+ 0.1 M NaOH	47.3	5.9×10^{-11}	5.4×10^{-13}
0.45 M Na_2SO_4+ 0.1 M NaOH	14.2	5.5×10^{-11}	4.9×10^{-13}

There are several ways in which salts can influence the transport of lignin through cellulose membranes: i) The presence of ions in the solution may alter the swelling behavior of the RC membrane, leading to changes in pore size and membrane thickness; ii) Lignin molecules tend to adsorb onto the membrane surface, which is influenced by the specific effects of ions, resulting in different behavior depending on the type of ion present; iii) The self-aggregation of lignin is also affected by the presence of ions in the solution, which could partially account for the variation in transport rates through the membrane.

The changes within the membrane (first point mentioned above) were studied by measuring the tritium-labeled water diffusivity through the membrane in various concentrations of $NaNO_3$, NaCl, and Na_2SO_4 salt solutions. While it is understood that the water diffusivity of the cellulose membrane does not only depend on the swelling of the membrane, the water diffusivity measurements provide us with an overall insight into how the membranes are affected by salts. Both water diffusivity and lignin diffusivity exhibited consistent trends across different solutions. While factors like lignin self-association, adsorption onto membrane

surfaces, and alterations in membrane thickness and pore sizes due to swelling could impact lignin diffusivity, water diffusivity is influenced by variations in membrane properties and solution characteristics. The presence of ions in the solution might induce changes in solution viscosity, subsequently influencing the mobility of water molecules within the solution.

The resemblance between the trends observed in water diffusivity and lignin diffusivity suggests that alterations to the cellulose membrane can have substantial consequences on the transport of lignin across the membrane (see Figure 2 d of Paper 3). The presence of salts can induce swelling in the cellulose membrane, which could result in the formation of tortuous and elongated diffusion pathways for lignin. Consequently, the available spaces for lignin diffusion might decrease. On the other hand, the swelling could also lead to an enlargement of the cellulose surface area, potentially providing more opportunities for lignin adsorption.

The second point, which is the adsorption of lignin in the presence of the selected salts from the Hofmeister series, was investigated using QCM-D. Figure 15 shows the adsorbed mass per area on the surface of the QCM-D sensors in the presence of different salts. Adsorption of lignin in the presence of nitrate ions was almost double that of the other investigated anions.

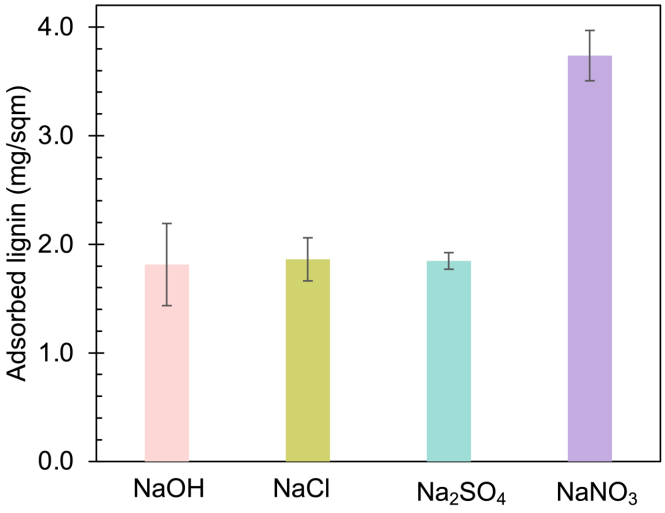

Figure 15 Average calculated adsorbed mass of lignin on the RC surface in the presence of different salts.

Adsorption of lignin on the cellulose substrate can occur through different mechanisms, such as van der Waals interactions, hydrogen bonding, or electrostatic interactions. In alkaline conditions, lignin molecules are negatively charged and the cellulose surface can also carry a negative net charge. Therefore, an electrostatic repulsion between the surface and lignin would be expected under these conditions. However, at higher salt concentrations, this electrostatic repulsion can be reduced, leading to adsorption promoted by non-electrostatic forces instead[81].

Current understanding suggests that the major driving force for adsorption is the entropy gain due to the release of water molecules from the interface during the process[134–137]. Anion-specific effects during adsorption are likely to originate from the differences in water organization at the interface in the presence of salts. As explained before, different ions have different hydrations that affect and alter the arrangement near the interface, affecting the adsorption process. Figure 16 is a schematic representation of how different ions can affect the adsorption of lignin.

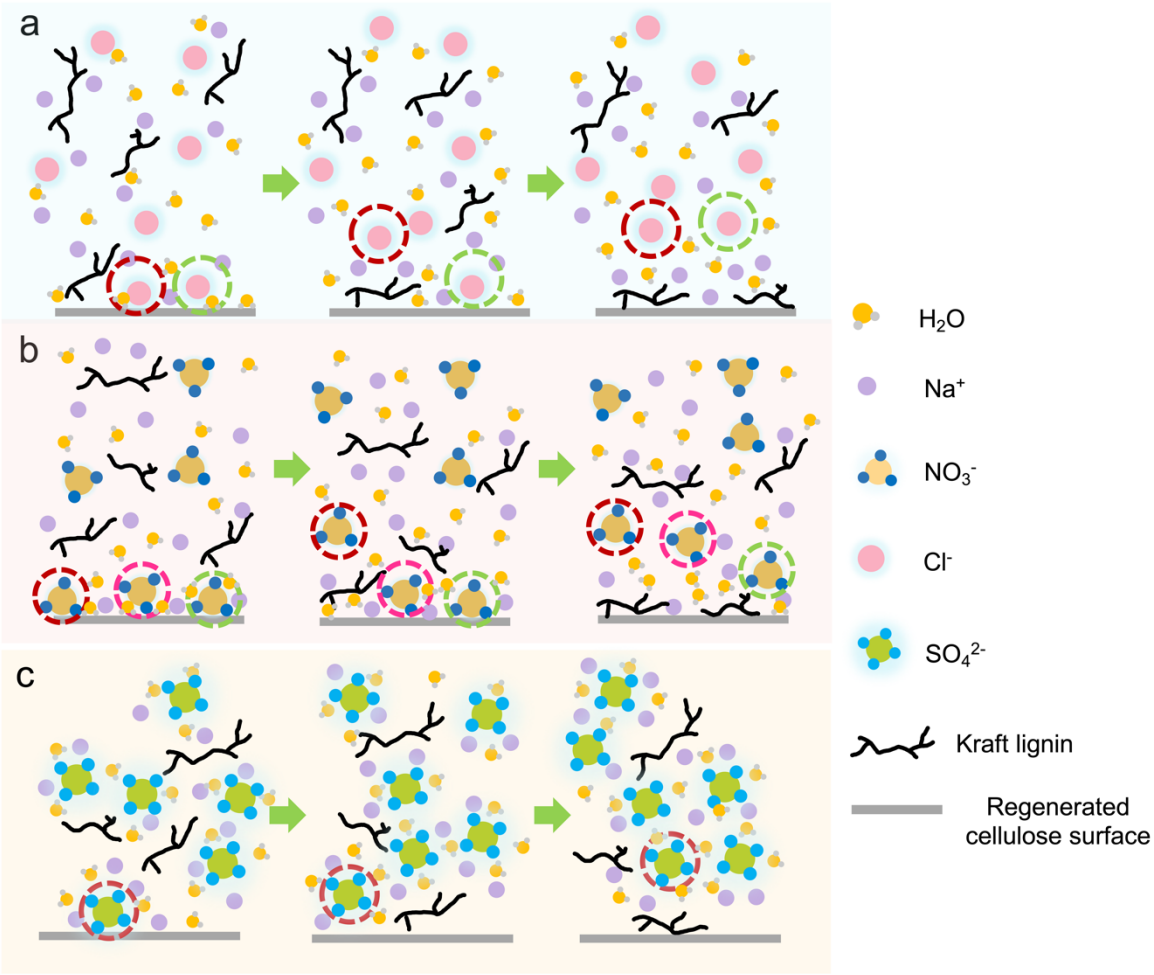

Figure 16 Illustration depicting lignin adsorption in the presence of different salts: a) NaCl, b) $NaNO_3$, and c) Na_2SO_4. The sequence from left to right demonstrates the arrangement of ions in the system. Notably, chaotropic (weakly hydrated) nitrate ions (b) tend to selectively organize themselves on the cellulose surface, while kosmotropic (highly hydrated) sulfate ions (c) are primarily distributed within the bulk water. The presence of nitrate ions on the surface prompts a more ordered configuration of water molecules near the membrane. Upon adsorption of lignin molecules onto the cellulose surface, the ions initially positioned on the surface are released into the surrounding solution. This ion release leads to an increase in the system's entropy.

4.2. Important parameters affecting mass transport of ionic liquids into wood

In every chemical pulping procedure, ensuring sufficient liquid penetration into the wood is of utmost importance. Attaining a uniform distribution of the active cooking chemicals throughout the voids within the wood chips is a crucial initial

step for the production of high-quality pulps. Ideally, each fiber within a wood chip undergoing pulping should experience an identical chemical treatment[7]. However, when it comes to separation processes based on ILs, the mass transport of these viscous liquids into the porous wood structure is challenging. In this thesis, the role of the impregnation step in delignification of wood pieces during the ionoSolv process was investigated. The concentrations of the released lignin molecules to the bulk liquid from a dry sample, an IL impregnated sample, and an IL impregnated and previously reacted sample were compared over time (Figure 17). Initially, the concentration of lignin released from the *impregnated-reacted* sample was higher than the other two samples since this sample already contained degraded lignin molecules in its structure, ready to diffuse out.

Throughout the course of the experiment, the lignin released from the *impregnated* sample and *impregnated-reacted* sample followed a similar trend. In contrast, the *dry* sample released much less lignin into the liquid compared to the other two. This highlights the critical role of the impregnation step. It implies that the mass transport of ILs into the wood structure could be a rate-limiting step in delignification.

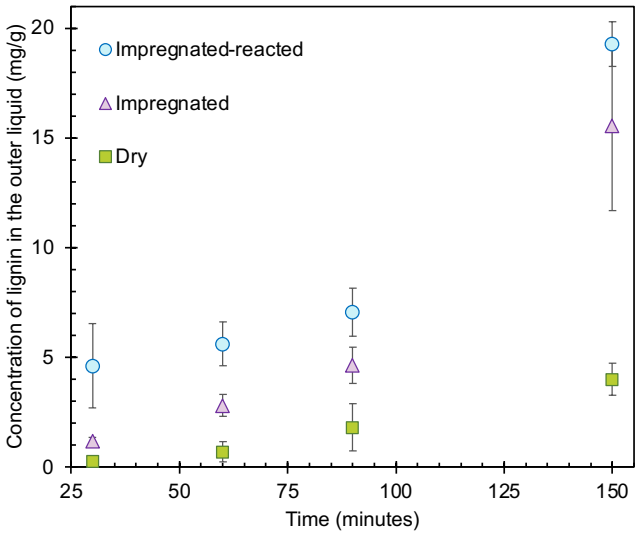

Figure 17 Concentration released lignin from different samples into the liquid over the course of the experiment.

Up to this point, the impact of the impregnation step on the rate of the process has been demonstrated. Recognizing the significance of this step in pulping, different factors like temperature, water content, and vacuum conditions, which can modify the impregnation process, were subsequently investigated.

Figure 18 shows how the wood pieces absorb the IL under different conditions after 30 minutes. The highest absorption of [DMBA][HSO_4] occurred when the wood pieces were placed in the IL containing 20% water, followed by maintaining them in a vacuum for 12 hours. The soaking continued for three days before their weight stopped increasing. The highest weight increase was approximately 2 times the weight of the initial dry wood, which is about 2 mL of the IL for the size of wood used (~ 1 x 1 x 3 cm).

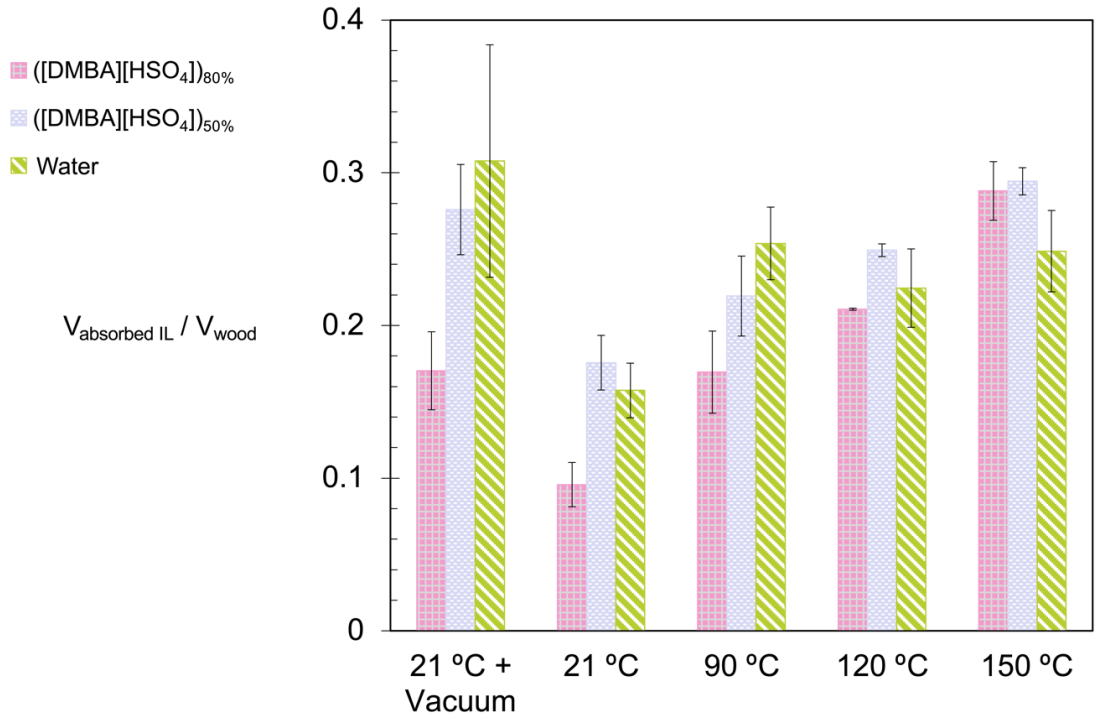

Figure 18 The ratio of the uptake of the IL by the wood pieces to the initial volume of the wood piece under different temperatures and water contents (20% water denoted by ($[DMBA][HSO_4]$)$_{80\%}$ and 50% water denoted by ($[DMBA][HSO_4]$)$_{50\%}$).

The difference in uptake between the samples exposed for 30 minutes and those saturated with IL indicates that achieving complete impregnation of wood pieces

of this size indeed requires more than 30 minutes. Complete impregnation includes two main mechanisms. The first is liquid penetration, which involves filling the empty spaces within the wood chip with liquid, driven by a pressure difference. This process is generally rapid. The second mechanism is the diffusion of chemicals into the fiber walls once the voids are filled. This diffusion mechanism relies on the concentration difference and is notably slower than the penetration process[138]. The presence of air within the empty spaces has been identified as a major hindrance to effectively saturating wood chips with liquid.

Consequently, eliminating air and evacuating the wood chips before impregnation has proven to be effective. Among the parameters that were studied here, vacuuming the desiccator while soaking the wood pieces in IL was shown to be the most effective (see Figure 18). A similar observation was made by Malkov et al., who reported better impregnation of wood chips when the chips were placed under vacuum for 5 minutes prior to soaking[64]. The higher uptake of water compared to the ILs can be explained by its lower viscosity, which means there is less resistance to its flow into the cavities.

In the experiments without a vacuum, the impregnation was enhanced by increasing temperature. Increasing temperature decreases the viscosity of liquids[139,140] which was desirable for the fluid flow and penetration of IL into tracheids. Indeed, viscosity seems to play an important role in the impregnation. Impregnation of wood pieces with the IL containing 20% water, $([DMBA][HSO_4])_{80\%}$, has consistently been less efficient than the 50% samples, $([DMBA][HSO_4])_{50\%}$, at all temperatures, with the main difference between these two ILs being their viscosity. The viscosity of the $([DMBA][HSO_4])_{50\%}$ was significantly lower than that of $([DMBA][HSO_4])_{80\%}$ at room temperature (4.6 mPa.s versus 44 mPa.s, see Paper 4)[140]. The difference in the liquid uptakes between samples was less significant as the temperature increased, reaching a negligible difference in the uptake liquid between the two IL samples at 150 °C.

Furthermore, diffusion increases proportionally with an increase in absolute temperature[63]. Therefore, higher temperatures are desirable for impregnation. However, once the temperature reaches 150 °C, the delignification reactions also start[52]. If the liquid is not homogeneously distributed within the wood chip, the degree of delignification between the surface of the wood and the middle of the wood might be different. Non-uniform delignification can complicate later stages such as saccharification or bleaching[141]. Hence, it is of utmost importance to find a balance between temperature, impregnation time, and water content. However, to achieve this, further investigations, such as finding the depth of penetration of IL within the wood piece as a function of time, viscosity and temperature, are required.

Chapter 5: Concluding Remarks

This thesis aimed to explore the significance of mass transport in pulping, driven by the difficulties encountered in existing pulping methods. As explained in this thesis, two steps in which mass transport is of vital importance are: i) transporting degraded products out of the fibers and ii) transporting active chemicals into wood.

The first model studies focused on the transport of lignin out of cellulose fibers. This was investigated using diffusion cells and model cellulose membranes. The results of the experiments revealed how different factors, such as confinement size, solution alkalinity, the molecular weight of lignin, and the presence of salts, affect the overall transport process.

It was observed that, when the confinements were small, the mass transport of dissolved lignin molecules slowed down significantly. This hints at how the diffusion of these molecules through fiber walls during pulping can markedly influence the overall rate of the process.

In cases of small confinements, molecule size plays a crucial role in their mass transport through the membrane. Hence, both the molecular weight of lignin molecules and the solution's alkalinity (which may alter the size of lignin clusters in the solution) influenced how efficiently mass was transferred through the cellulose pores. Expectedly, by increasing the alkalinity of the solution, the association between lignin molecules diminished, which led to a more efficient transport through pores.

In addition, the behavior of charged lignin molecules when interacting with sodium salts from the Hofmeister series was studied. This opened up a door to the world of specific ion effects. These effects became particularly evident when lignin adsorption to the cellulose surface was increased in the presence of nitrate. QCM-D measurements were used to capture this interaction. The adsorption process

seems to be driven by the system's entropy gain due to the rearrangement of water molecules at the surface upon lignin's adsorption.

Finally, the importance of mass transport in a novel biomass pretreatment process, ionoSolv, was highlighted in the final study. A method for studying the rate-limiting step in ionoSolv was developed. It was observed that significantly less lignin was released into the outer liquid when the IL was not transported into the wood structure prior to the reactions. The results emphasized the importance of having an efficient impregnation process on the delignification process. They suggest that the mass transport of chemicals into the wood structure is the rate-determining step. The rest of the study was, therefore, focused on finding desirable conditions for improving impregnation. Wood pieces were subjected to various conditions (different temperatures, water contents, and the presence of a vacuum). Higher temperature and higher water content seem to improve impregnation, which points out the role of the viscosity of the solution on impregnation. In conclusion, this thesis provides fundamental information about mass transport events in wood disintegration while acknowledging their complexity.

Chapter 6: Future Outlook

Despite the progress made in our present comprehension of mass transport events in pulping, there remain aspects that necessitate further investigation and refinement. One of these aspects is how the presence and concentration of salts in solution affects the cellulose fibers, with regards to swelling, etc. This thesis has undertaken attempts to understand the alterations within the cellulose membrane using the water diffusion experiments. While these experiments provide an overall impression of how the membrane was affected in each solution, the systematic study of the degree to which the membrane swells would provide added value. One viable method to study the swelling of cellulose in the presence of salts is by using the same QCM-D methods and recording the change in frequency and dissipation of the coated surface in response to changing the salt solutions and their concentrations.

The importance of impregnation in ionoSolv pretreatment and how various parameters can affect the efficient impregnation of wood pieces was also highlighted. However, it is vital to examine the depth of penetration of the ILs into wood pieces and the homogeneity of their distribution in the various studied conditions. The presence and concentration of ILs in the wood pieces can be identified using techniques such as scanning electron microscopy with energy-dispersive x-ray spectroscopy (SEM-EDX) or IR-microscopy. It is also of great importance to identify where ILs are located within the cell walls in various sections of the wood pieces.

This thesis also explored how higher temperature improves impregnation. High temperatures, such as 150 °C, also start the delignification reactions wherever the IL is in contact. This leads to high delignification starting on the surface of the wood piece, where the IL is in direct contact ,while the inside of the piece is still

dry. Hence, further studies are needed to find an optimum balance between water content, vacuum, and temperature.

Lastly, structural changes within the wood pieces after treatment with the IL were observed. While some damages to the structure were obvious, whether or not this IL ([DMBA][HSO_4]) swells the structure could not be identified, nor could the extent to which it affects the cellulose fibers if the structure does swell. Hence a study on the ability of [DMBA][HSO_4] to swell wood is essential.

Chapter 7: Acknowledgements

The financial support for this project has been graciously provided by the Knut and Alice Wallenberg Foundation through the Wallenberg Wood Science Center (WWSC) and I would like to extend my sincere appreciation for their generosity.

The past years have truly been the most remarkable period of my academic life. During these years, many wonderful individuals supported me and encouraged me to grow into a better researcher. Hereby, I want to acknowledge their support during this amazing journey.

To begin, I would like to express my sincere gratitude to my main supervisor, Prof. Anette Larsson. Thank you for believing in me, patiently listening to me, and for providing me with the opportunity to grow. Your support and friendship have been truly invaluable during these years.

I would like to extend my genuine thanks to my supervision team, my former examiner, Prof. Hans Theliander, my co-supervisor, Prof. Martin Lawoko, and my current examiner, Prof. Christian Müller, for their support and fruitful scientific discussions.

I am truly thankful to all my co-authors and collaborators. Especially Prof. Gunnar Lidén for welcoming me to his lab at Lund University. The week I spent in their group truly made its mark on my Ph.D. journey. Furthermore, I am very grateful for our collaboration with the Lixea company and its amazing scientific team, Dr. Florence Gschwend, Dr. Agnieszka Brandt-Talbot, and Prof. Jason Hallett from the Imperial College of London. I have learned greatly from each one of you.

This Ph.D. journey would have been far less enriching without the unwavering support of my friends and colleagues at Chalmers. My heartfelt gratitude extends to all the present and former members of the LNS group – thank you for being

incredible groupmates. I'm deeply thankful to my officemates at the Applied Chemistry division, including Marika, Robin, Åke, and Bagus, for patiently listening to my frustrations and sharing in all the fun activities.

I'd like to express my appreciation to my WWSC fellow Ph.D. students: Kenneth, for his unwavering support, Ehsan, for the enjoyable conversations, and Sozan, for adding a touch of awesomeness to my days.

Furthermore, I'm very grateful to my dear friends and colleagues, Rydvikha, Vishnu, and Marina, for their invaluable guidance and wisdom at various stages of my Ph.D. journey.

I want to express my wholehearted thanks to my best friend, Yasaman. Thanks a million for keeping the encouragement flowing, even when our location pins were miles apart. You're a real champion in the friendship game!

I want to express my heartfelt thanks to my amazing partner, Amir. Your constant support, both emotionally and scientifically, has been an incredible gift. It's truly special to have a best friend, life partner, and science buddy all rolled into one fantastic person like you.

Sweden began to feel like home with the warmth of my wonderful Iranian friends, Nima, Pantea, Tina and Shahrzad. I am immensely grateful for their friendship.

Last but certainly not least, I want to thank my beloved family. I extend my heartfelt gratitude to my mother, Sousan, who was a constant source of inspiration on this educational journey. To my father, Mehran, whose contagious interest in science fueled my passion. To my brother, Arjang, who brought bundles of joy to our family. And to my grandmother, Fatemeh, who has been my rock throughout it all. Words cannot encompass the depth of my appreciation for each one of you.

References

1. Perlack, R.D., Wright, L.L., Turhollow, A.F., Graham, R. L. Biomass as Feedstock for a Bioenergy and Bioproducts Industry : The Technical Feasibility of a Billion-Ton Annual Supply. *Agriculture* 1–78 (2005). doi:10.2172/885984

2. Antizar-Ladislao, B. & Turrion-Gomez, J. L. Second-generation biofuels and local bioenergy systems. *Biofuels, Bioprod. Biorefining* **2**, 455–469 (2008).

3. Monica Ek, Göran Gellerstedt, G. H. & Höglund, H. Mechanical pulping. *Pulping Chem. Technol.* **22**, 57 (2009).

4. Mboowa, D. A review of the traditional pulping methods and the recent improvements in the pulping processes. *Biomass Convers. Biorefinery* (2021). doi:10.1007/s13399-020-01243-6

5. Ragnar, M. *et al.* Ullmann's Encyclopedia of Industrial Chemistry. *Ullmann's encyclopedia of industrial chemistry* (2014). doi:https://doi.org/10.1002/14356007.a18_545.pub4

6. Rabelo, S. C. *et al.* Organosolv pretreatment for biorefineries: Current status, perspectives, and challenges. *Bioresour. Technol.* **369**, (2023).

7. Sixta, H. *Handbook of the pulp*. (2006).

8. del Mar Contreras-Gámez, M. *et al.* Deep eutectic solvents for improved biomass pretreatment: Current status and future prospective towards sustainable processes. *Bioresour. Technol.* **369**, (2023).

9. Cheremisinoff, N. P. & Rosenfeld, P. E. Sources of air emissions from pulp and paper mills. *Handb. Pollut. Prev. Clean. Prod.* **2**, 179–259 (2010).

10. Dahl, C. F. Process of manufacturing cellulose from wood. *US Pat. Off.*

https://patents.google.com/patent/US296935A (1884).

11. Stratton, S. C., Gleadow, P. L. & Johnson, A. P. Pulp mill process closure: A review of global technology developments and mill experiences in the 1990s. *Water Sci. Technol.* **50**, 183–194 (2004).

12. Kumar, H. & Christopher, L. P. Recent trends and developments in dissolving pulp production and application. *Cellulose* **24**, 2347–2365 (2017).

13. Macleod, J. M. & MacLeod, M. Where are bleached Kraft Mills going? Brighter? Cleaner? Cheaper? *RISI Pulp Pap. Mag.* (2008).

14. Brandt, A. *et al.* Ionic liquid pretreatment of lignocellulosic biomass with ionic liquid–water mixtures. *Green Chem.* **13**, 2489–2499 (2011).

15. George, A. *et al.* Design of low-cost ionic liquids for lignocellulosic biomass pretreatment. *Green Chem.* **17**, 1728–1734 (2015).

16. Brandt, A., Gräsvik, J., Hallett, J. P. & Welton, T. Deconstruction of lignocellulosic biomass with ionic liquids. *Green Chem.* **15**, 550–583 (2013).

17. Brandt, A., Hallett, J. P., Leak, D. J., Murphy, R. J. & Welton, T. The effect of the ionic liquid anion in the pretreatment of pine wood chips. *Green Chem.* **12**, 672–67 (2010).

18. Abouelela, A. R., Nakasu, P. Y. S. & Hallett, J. P. Influence of Pretreatment Severity Factor and Hammett Acidity on Softwood Fractionation by an Acidic Protic Ionic Liquid. *ACS Sustain. Chem. Eng.* **11**, 2404–2415 (2023).

19. Radkau, J. *Wood: a history*. (Polity, 2012).

20. Milks, A. *et al. A double-pointed wooden throwing stick from Schöningen, Germany: Results and new insights from a multianalytical study*. *PloS one* **18**, (2023).

21. Hall, F. K. Wood Pulp. *Sci. Am.* **230**, 52–65 (1974).

22. Wang, J., Wang, L., Gardner, D. J., Shaler, S. M. & Cai, Z. *Towards a cellulose-based society: opportunities and challenges*. *Cellulose* **28**, (Springer Netherlands, 2021).

23. Felgueiras, C., Azoia, N. G., Gonçalves, C., Gama, M. & Dourado, F. Trends on the Cellulose-Based Textiles: Raw Materials and Technologies. *Front. Bioeng. Biotechnol.* **9**, 1–20 (2021).

24. Bledzki, A. K. & Gassan, J. Composites reinforced with cellulose based fibres. *Prog. Polym. Sci.* **24**, 221–274 (1999).

25. Miao, C. & Hamad, W. Y. Cellulose reinforced polymer composites and nanocomposites: A critical review. *Cellulose* **20**, 2221–2262 (2013).

26. Siddiqa, A. *et al.* Review and Perspectives of Sustainable Lignin, Cellulose, and Lignocellulosic Carbon Special Structures for Energy Storage. *Energy and Fuels* **37**, 2498–2519 (2023).

27. Chen, W. *et al.* Nanocellulose: A promising nanomaterial for advanced electrochemical energy storage. *Chem. Soc. Rev.* **47**, 2837–2872 (2018).

28. Obasa, V. D. *et al.* A Review on Lignin-Based Carbon Fibres for Carbon Footprint Reduction. *Atmosphere (Basel).* **13**, (2022).

29. Rajesh Banu, J. *et al.* A review on biopolymer production via lignin valorization. *Bioresour. Technol.* **290**, 121790 (2019).

30. Sjöström, E. *Wood chemistry, fundamentals and applications*. *Academic press, Inc* (1993). doi:10.1016/0008-6215(94)90030-2

31. Sjöström, E. Chapter 1 - THE STRUCTURE OF WOOD. in *Wood Chemistry* (ed. SJÖSTRÖM, E. B. T.-W. C. (Second E.) 1–20 (Academic Press, 1993). doi:https://doi.org/10.1016/B978-0-08-092589-9.50005-X

32. Gatenholm, P. & Tenkanen, M. *Hemicelluloses: science and technology*.

(ACS Publications, 2003).

33. Candolle, D. & SJÖSTRÖM, E. Chapter 4 - LIGNIN. in (ed. SJÖSTRÖM, E. B. T.-W. C. (Second E.) 71–89 (Academic Press, 1993). doi:https://doi.org/10.1016/B978-0-08-092589-9.50008-5

34. Lawoko, M., Henriksson, G. & Gellerstedt, G. Structural differences between the lignin-carbohydrate complexes present in wood and in chemical pulps. *Biomacromolecules* **6**, 3467–3473 (2005).

35. Zhao, X., Cheng, K. & Liu, D. Organosolv pretreatment of lignocellulosic biomass for enzymatic hydrolysis. *Appl. Microbiol. Biotechnol.* **82**, 815–827 (2009).

36. Usmani, Z. *et al.* Ionic liquid based pretreatment of lignocellulosic biomass for enhanced bioconversion. *Bioresour. Technol.* **304**, 123003 (2020).

37. Chen, Y. & Mu, T. Application of deep eutectic solvents in biomass pretreatment and conversion. *Green Energy Environ.* **4**, 95–115 (2019).

38. Chemistry, C. & Tomani, P. The lignoboost process. (2015).

39. Mattsson, C., Hasani, M., Dang, B., Mayzel, M. & Theliander, H. About structural changes of lignin during kraft cooking and the kinetics of delignification. *Holzforschung* **71**, 545–553 (2017).

40. Dang, B. T. T., Brelid, H. & Theliander, H. The impact of ionic strength on the molecular weight distribution (MWD) of lignin dissolved during softwood kraft cooking in a flow-through reactor. *Holzforschung* **70**, 495–501 (2016).

41. Hallett, J. P. & Welton, T. Room-temperature ionic liquids: Solvents for synthesis and catalysis. 2. *Chem. Rev.* **111**, 3508–3576 (2011).

42. Wang, X., Li, H., Cao, Y. & Tang, Q. Cellulose extraction from wood chip in an ionic liquid 1-allyl-3-methylimidazolium chloride (AmimCl). *Bioresour.*

Technol. **102**, 7959–7965 (2011).

43. Pinkert, A., Marsh, K. N., Pang, S. & Staiger, M. P. Ionic liquids and their interaction with cellulose. *Chem. Rev.* **109**, 6712–6728 (2009).

44. Chen, L. *et al.* Inexpensive ionic liquids: [HSO4]--based solvent production at bulk scale. *Green Chem.* **16**, 3098–3106 (2014).

45. Clough, M. T., Geyer, K., Hunt, P. A., Mertes, J. & Welton, T. Thermal decomposition of carboxylate ionic liquids: Trends and mechanisms. *Phys. Chem. Chem. Phys.* **15**, 20480–20495 (2013).

46. Viell, J. *et al.* Multi-scale processes of beech wood disintegration and pretreatment with 1-ethyl-3-methylimidazolium acetate/water mixtures. *Biotechnol. Biofuels* **9**, 1–15 (2016).

47. Swatloski, R. P., Spear, S. K., Holbrey, J. D. & Rogers, R. D. Dissolution of cellose with ionic liquids. *J. Am. Chem. Soc.* **124**, 4974–4975 (2002).

48. Gschwend, F. J. V. *et al.* Quantitative glucose release from softwood after pretreatment with low-cost ionic liquids. *Green Chem.* **21**, 692–703 (2019).

49. Weigand, L., Mostame, S., Brandt-Talbot, A., Welton, T. & Hallett, J. P. Effect of pretreatment severity on the cellulose and lignin isolated from: Salix using ionoSolv pretreatment. *Faraday Discuss.* **202**, 331–349 (2017).

50. Chambon, C. L. *et al.* Pretreatment of south african sugarcane bagasse using a low-cost protic ionic liquid: A comparison of whole, depithed, fibrous and pith bagasse fractions. *Biotechnol. Biofuels* **11**, 1–16 (2018).

51. Anuchi, S. O., Campbell, K. L. S. & Hallett, J. P. Effective pretreatment of lignin-rich coconut wastes using a low-cost ionic liquid. *Sci. Rep.* **12**, 1–11 (2022).

52. Gschwend, F. J. V., Malaret, F., Shinde, S., Brandt-Talbot, A. & Hallett, J.

P. Rapid pretreatment of: Miscanthus using the low-cost ionic liquid triethylammonium hydrogen sulfate at elevated temperatures. *Green Chem.* **20**, 3486–3498 (2018).

53. Shi, J. *et al.* Understanding the role of water during ionic liquid pretreatment of lignocellulose: Co-solvent or anti-solvent? *Green Chem.* **16**, 3830–3840 (2014).

54. Gschwend, F. J. V. *et al.* Towards an environmentally and economically sustainable biorefinery: heavy metal contaminated waste wood as a low-cost feedstock in a low-cost ionic liquid process. *Green Chem.* **22**, 5032–5041 (2020).

55. Brandt-Talbot, A. *et al.* An economically viable ionic liquid for the fractionation of lignocellulosic biomass. *Green Chem.* **19**, 3078–3102 (2017).

56. Brännvall, E. The Limits of Delignification in Kraft Cooking. *BioResources* **12**, 2081–2107 (2017).

57. Bogren, J., Brelid, H. & Theliander, H. Reaction kinetics of softwood kraft delignification - General considerations and experimental data. *Nord. Pulp Pap. Res. J.* **22**, 177–183 (2007).

58. Li, J. & Mui, C. Effect of lignin diffusion on kraft delignification kinetics as determined by liquor analysis. Part I: An experimental study. *J. Pulp Pap. Sci.* **25**, 373–377 (1999).

59. Simão, J. P. F., Egas, A. P. V., Carvalho, M. G. V. S., Baptista, C. M. S. G. & Castro, J. A. A. M. Heterogeneous studies in pulping of wood: Modelling mass transfer of alkali. *Chem. Eng. J.* **139**, 615–621 (2008).

60. Egas, A. P. V., Simão, J. P. F., Costa, I. M. M., Francisco, S. C. P. & Castro, J. A. A. M. Experimental methodology for heterogeneous studies in pulping of wood. *Ind. Eng. Chem. Res.* **41**, 2529–2534 (2002).

61. Wedin, H., Lindström, M. E., Ragnar, M. & Kommun, H. Extended impregnation in the kraft cook - An approach to improve the overall yield in eucalypt kraft pulping. *Nord. Pulp Pap. Res. J.* **25**, 7–14 (2010).

62. Wedin, H., Fiskari, J., Kovasin, K., Ragnar, M. & Lindström, M. E. Further insights into extended-impregnation kraft cooking of birch. *Nord. Pulp Pap. Res. J.* **27**, 890–899 (2012).

63. Cussler, E. L. *Diffusion: mass transfer in fluid systems*. (Cambridge university press, 2009).

64. Malkov, S., Tikka, P. & Gullichsen, J. Towards complete impregnation of wood chips with aqueous solutions: part 2. Studies on water penetration into softwood chips. *Pap. ja Puu/Paper Timber* **83**, 468–473 (2001).

65. Cable, M. & Frade, J. R. The Influence of Surface Tension on the Diffusion-Controlled Growth or Dissolution of Spherical Gas Bubbles. *Proc. R. Soc. Lond. A. Math. Phys. Sci.* **420**, 247–265 (1988).

66. Malkov, S., Tikka, P. & Gullichsen, J. Towards complete impregnation of wood chips with aqueous solutions: Part 3. Black liquor penetration into pine chips. *Pap. ja Puu/Paper Timber* **83**, 605–609 (2001).

67. Lönnberg, B. Pre-impregnation of wood chips for alkaline delignification. *Cellul. Chem. Technol.* **50**, 675–680 (2016).

68. Brännvall, E. & Bäckström, M. Improved impregnation efficiency and pulp yield of softwood kraft pulp by high effective alkali charge in the impregnation stage. *Holzforschung* **70**, 1031–1037 (2016).

69. Perko, J. *et al.* The importance of physical parameters for the penetration depth of impregnation products into cementitious materials: Modelling and experimental study. *Constr. Build. Mater.* **257**, (2020).

70. Kazi, K. M. F., Gauvin, H., Jollez, P. & Chornet, E. A diffusion model for the

impregnation of lignocellulosic materials. *Tappi J.* **80**, 209–219 (1997).

71. Hart, P. W., Colson, G. W., Antonsson, S. & Hjort, A. Impact of impregnation on high kappa number hardwood pulps. *BioResources* **6**, 5139–5150 (2011).

72. Aid, T., Hyvärinen, S., Vaher, M., Koel, M. & Mikkola, J. P. Saccharification of lignocellulosic biomasses via ionic liquid pretreatment. *Ind. Crops Prod.* **92**, 336–341 (2016).

73. Mosier, N. *et al.* Features of promising technologies for pretreatment of lignocellulosic biomass. *Bioresour. Technol.* **96**, 673–686 (2005).

74. Brännvall, E. & Rönnols, J. Analysis of entrapped and free liquor to gain new insights into kraft pulping. *Cellulose* **28**, 2403–2418 (2021).

75. Eriksson, G. & Grén, U. Pulp washing: Influence of temperature on lignin leaching from kraft pulps. *Nord. Pulp Pap. Res. J.* **12**, 244–251 (1997).

76. Favis, B. D., Choi, P. M. K., Adler, P. M. & Goring, D. A. I. Leaching of lignin from unbleached kraft fibers suspended in water.pdf. *Pulp Pap. CANADA* **82**, TR35–TR40 (1981).

77. Li, J. & Macleod, J. M. Alkaline Leaching of Kraft Pulps For Lignin Removal. *J. Pulp Pap. Sci.* **19**, 85–92 (1993).

78. Li, J., Phoenix, A. & Macleod, J. M. Diffusion of Lignin Macromolecules Within the Fibre Walls of Kraft Pulp. Part I: Determination of the Diffusion Coefficient under Alkaline Conditions. *Can. J. Chem. Eng.* **75**, 16–22 (1997).

79. Norgren, M., Edlund, H., Wågberg, L., Lindström, B. & Annergren, G. Aggregation of kraft lignin derivatives under conditions relevant to the process, part I: Phase behaviour. *Colloids Surfaces A Physicochem. Eng. Asp.* **194**, 85–96 (2001).

80. Bogren, J., Brelid, H., Bialik, M. & Theliander, H. Impact of dissolved

sodium salts on kraft cooking reactions. *Holzforschung* **63**, 226–231 (2009).

81. van de Steeg, H. G. M., Stuart, M. A. C., de keizer, A. & Bijsterbosch, B. H. Polyelectrolyte Adsorption: A Subtle Balance of Forces. *Langmuir* **8**, 2538–2546 (1992).

82. Helmholtz, H. Der phystk und chemie. 1. *Ann. der Phys. und Chemie* **165**, 353–377 (1853).

83. Grahame, D. C. The Electrical Double Layer and the Theory of Electrocapillarity. *Chem. Rev.* **41**, 441–501 (1947).

84. Gouy, M. Sur la constitution de la charge électrique à la surface d'un électrolyte. *J. Phys. Théorique Appliquée* **9**, 457–468 (1910).

85. Chapman, D. L. LI. A contribution to the theory of electrocapillarity . *London, Edinburgh, Dublin Philos. Mag. J. Sci.* **25**, 475–481 (1913).

86. Stern, O. Zur Theorie der elektrolytischen Ventilwirkung. *Zeitschrift für Electrochem. und Angw. Phys, Chemie* **30**, 508 (1924).

87. Berg, J. C. An Introduction to Interfaces and Colloids The Bridge to Nanoscience World Scientific. (2010).

88. Marcus, Y. Effect of ions on the structure of water. *Pure Appl. Chem.* **82**, 1889–1899 (2010).

89. Boström, M., Kunz, W. & Ninham, B. W. Hofmeister effects in surface tension of aqueous electrolyte solution. *Langmuir* **21**, 2619–2623 (2005).

90. Zhang, Y. & Cremer, P. S. Interactions between macromolecules and ions: the Hofmeister series. *Curr. Opin. Chem. Biol.* **10**, 658–663 (2006).

91. Kherb, J., Flores, S. C. & Cremer, P. S. Role of carboxylate side chains in the cation hofmeister series. *J. Phys. Chem. B* **116**, 7389–7397 (2012).

92. Chen, X., Yang, T., Kataoka, S. & Cremer, P. S. Specific ion effects on interfacial water structure near macromolecules. *J. Am. Chem. Soc.* **129**, 12272–12279 (2007).

93. Aroti, A., Leontidis, E., Maltseva, E. & Brezesinski, G. Effects of hofmeister anions on DPPC langmuir monolayers at the air-water interface. *J. Phys. Chem. B* **108**, 15238–15245 (2004).

94. Hofmeister, F. Zur Lehre von der Wirkung der Salze - Dritte Mittheilung. *Arch. für Exp. Pathol. und Pharmakologie* **25**, 1–30 (1888).

95. Kunz, W., Henle, J. & Ninham, B. W. 'Zur Lehre von der Wirkung der Salze' (about the science of the effect of salts): Franz Hofmeister's historical papers. *Curr. Opin. Colloid Interface Sci.* **9**, 19–37 (2004).

96. Okur, H. I. *et al.* Beyond the Hofmeister Series: Ion-Specific Effects on Proteins and Their Biological Functions. *J. Phys. Chem. B* **121**, 1997–2014 (2017).

97. Collins, K. D. Why continuum electrostatics theories cannot explain biological structure, polyelectrolytes or ionic strength effects in ion-protein interactions. *Biophys. Chem.* **167**, 43–59 (2012).

98. Collins, K. D. Charge density-dependent strength of hydration and biological structure. *Biophys. J.* **72**, 65–76 (1997).

99. Marcus, Y. & Hefter, G. Ion pairing. *Chem. Rev.* **106**, 4585–4621 (2006).

100. Boström, M., Williams, D. R. M. & Ninham, B. W. Specific ion effects: Why DLVO theory fails for biology and colloid systems. *Phys. Rev. Lett.* **87**, 168103/1-168103/4 (2001).

101. Ninham, B. W. & Yaminsky, V. Ion binding and ion specificity: The Hofmeister effect and Onsager and Lifshitz theories. *Langmuir* **13**, 2097–2108 (1997).

102. Lifshitz, R. & Petrich, D. M. Theoretical model for faraday waves with multiple-frequency forcing. *Phys. Rev. Lett.* **79**, 1261–1264 (1997).

103. Boström, M., Williams, D. R. M. & Ninham, B. W. The influence of ionic dispersion potentials on counterion condensation on polyelectrolytes. *J. Phys. Chem. B* **106**, 7908–7912 (2002).

104. Boström, M. & Ninham, B. W. Why pH titration in lysozyme suspensions follow a Hofmeister series. *Colloids Surfaces A Physicochem. Eng. Asp.* **291**, 24–29 (2006).

105. Salis, A. *et al.* Specific anion effects on glass electrode ph measurements of buffer solutions: Bulk and surface phenomena. *J. Phys. Chem. B* **110**, 2949–2956 (2006).

106. Boström, M., Williams, D. R. M. & Ninham, B. W. Surface tension of electrolytes: Specific ion effects explained by dispersion forces. *Langmuir* **17**, 4475–4478 (2001).

107. Van den Mooter, G., Samyn, C. & Kinget, R. Characterization of colon-specific azo polymers: A study of the swelling properties and the permeability of isolated polymer films. *Int. J. Pharm.* **111**, 127–136 (1994).

108. Nilsson, R., Olsson, M., Westman, G., Matic, A. & Larsson, A. Screening of hydrogen bonds in modified cellulose acetates with alkyl chain substitutions. *Carbohydr. Polym.* **285**, 119188 (2022).

109. Andersson, H., Hjärtstam, J., Stading, M., Von Corswant, C. & Larsson, A. Effects of molecular weight on permeability and microstructure of mixed ethyl-hydroxypropyl-cellulose films. *Eur. J. Pharm. Sci.* **48**, 240–248 (2013).

110. Liu, Z., Choi, H., Gatenholm, P. & Esker, A. R. Quartz Crystal Microbalance with Dissipation Monitoring and Surface Plasmon Resonance Studies of Carboxymethyl Cellulose Adsorption onto Regenerated Cellulose Surfaces.

Sect. Title Surf. Chem. Colloids (2011). doi:10.1021/la200628a

111. Kargl, R. *et al.* Adsorption of carboxymethyl cellulose on polymer surfaces: Evidence of a specific interaction with cellulose. *Langmuir* (2012). doi:10.1021/la302110a

112. Naderi, A. & Claessont, P. M. Adsorption properties of polyelectrolyte-surfactant complexes on hydrophobic surfaces studied by QCM-D. *Langmuir* **22**, 7639–7645 (2006).

113. Mohan, T. *et al.* Wettability and surface composition of partly and fully regenerated cellulose thin films from trimethylsilyl cellulose. *J. Colloid Interface Sci.* **358**, 604–610 (2011).

114. Duval, A., Vilaplana, F., Crestini, C. & Lawoko, M. Solvent screening for the fractionation of industrial kraft lignin. *Holzforschung* **70**, 11–20 (2016).

115. Fahlén, J. & Salmén, L. Cross-sectional structure of the secondary wall of wood fibers as affected by processing. *J. Mater. Sci.* **38**, 119–126 (2003).

116. Aksenov, A. S. *et al.* Biocatalysis of industrial kraft pulps: Similarities and differences between hardwood and softwood pulps in hydrolysis by enzyme complex of penicillium verruculosum. *Catalysts* **10**, (2020).

117. Rudatin, S., Sen, Y. L. & Woerner, D. L. Association of Kraft Lignin in Aqueous Solution. in *Lignin* **397**, 11–144 (American Chemical Society, 1989).

118. Gärtner, A., Gellerstedt, G. & Tamminen, T. Determination of phenolic hydroxyl groups in residual lignin using a modified UV-method. *Nord. Pulp Pap. Res. J.* **14**, 163–170 (1999).

119. Zakis, G. F. *Functional analysis of lignins and their derivatives*. (Tappi Press, 1994).

120. Y.Lin, S. & Dence, C. W. *Methods in Lignin Chemistry*. *Journal of Chemical*

Information and Modeling **53**, (1992).

121. Goldmann, W. M. *et al.* Determination of phenolic hydroxyl groups in technical lignins by ionization difference ultraviolet spectrophotometry (Δε-IDUS method). *Period. Polytech. Chem. Eng.* **61**, 93–101 (2017).

122. Heitner, C., Dimmel, D. R. & Schmidt, J. A. *Lignin and lignans, Advances in chemistry*. *Lignin and Lignans* (2010). doi:10.1201/ebk1574444865-c2

123. Tiainen, E., Drakenberg, T., Tamminen, T., Kataja, K. & Hase, A. Determination of phenolic hydroxyl groups in lignin by combined use of1H NMR and UV spectroscopy. *Holzforschung* **53**, 529–533 (1999).

124. Klein, J. Dynamics of Entangled Linear, Branched, and Cyclic Polymers. *Macromolecules* **19**, 105–118 (1986).

125. De Gennes, P. G. Reptation of a polymer chain in the presence of fixed obstacles. *J. Chem. Phys.* **55**, 572–579 (1971).

126. Grignon, J. & Scallan, A. M. Effect of pH and neutral salts upon the swelling of cellulose gels. *J. Appl. Polym. Sci.* **25**, 2829–2843 (1980).

127. Norgren, M. & Bergfors, E. Sorption of kraft lignin from spent liquors on pulp fibres. *Wood Sci. Technol.* **39**, 512–520 (2005).

128. Norgren, M. & Lindström, B. Dissociation of phenolic groups in kraft lignin at elevated temperatures. *Holzforschung* **54**, 519–527 (2000).

129. Bikova, T., Treimanis, A., Rossinska, G. & Telysheva, G. On-line study of lignin behaviour in dilute alkaline solution by the SEC-UV method. *Holzforschung* **58**, 489–494 (2004).

130. Norgren, M. & Edlund, H. Ion specific differences in salt induced precipitation of kraft lignin. *Nord. Pulp Pap. Res. J.* **18**, 400–403 (2003).

131. Chudoba, R., Heyda, J. & Dzubiella, J. Tuning the collapse transition of

weakly charged polymers by ion-specific screening and adsorption. *Soft Matter* **14**, 9631–9642 (2018).

132. Rogers, B. A. *et al.* Weakly hydrated anions bind to polymers but not monomers in aqueous solutions. *Nat. Chem.* **14**, 40–45 (2022).

133. Bruce, E. E. *et al.* Molecular mechanism for the interactions of hofmeister cations with macromolecules in aqueous solution. *J. Am. Chem. Soc.* **142**, 19094–19100 (2020).

134. Benselfelt, T. *et al.* Adsorption of Xyloglucan onto Cellulose Surfaces of Different Morphologies: An Entropy-Driven Process. *Biomacromolecules* **17**, 2801–2811 (2016).

135. Kishani, S., Benselfelt, T., Wågberg, L. & Wohlert, J. Entropy drives the adsorption of xyloglucan to cellulose surfaces – A molecular dynamics study. *J. Colloid Interface Sci.* **588**, 485–493 (2021).

136. Arumughan, V., Nypelö, T., Hasani, M. & Larsson, A. Calcium Ion-Induced Structural Changes in Carboxymethylcellulose Solutions and Their Effects on Adsorption on Cellulose Surfaces. *Biomacromolecules* **23**, 47–56 (2022).

137. Arumughan, V., Nypelö, T., Hasani, M. & Larsson, A. Fundamental aspects of the non-covalent modification of cellulose via polymer adsorption. *Adv. Colloid Interface Sci.* **298**, (2021).

138. Stone, J. E. & Forderreuther, C. Studies of penetration and diffusion into wood. *Tappi* **39**, 679 (1956).

139. Belieres, J. P. & Angell, C. A. Protic ionic liquids: Preparation, characterization, and proton free energy level representation. *J. Phys. Chem. B* **111**, 4926–4937 (2007).

140. Malaret, F. J. En route to the industrial applications of ionic liquids for metal oxide production and biomass fractionation: A sustainable avenue to

advanced materials. (Imperial College of London, 2020).

141. Rydholm, S. A. Pulping processes. *Pulping Process.* (1965).